

**Manuscript version: Author's Accepted Manuscript**

The version presented in WRAP is the author's accepted manuscript and may differ from the published version or Version of Record.

**Persistent WRAP URL:**

<http://wrap.warwick.ac.uk/141032>

**How to cite:**

Please refer to published version for the most recent bibliographic citation information. If a published version is known of, the repository item page linked to above, will contain details on accessing it.

**Copyright and reuse:**

The Warwick Research Archive Portal (WRAP) makes this work by researchers of the University of Warwick available open access under the following conditions.

© 2020 Elsevier. Licensed under the Creative Commons Attribution-NonCommercial-NoDerivatives 4.0 International <http://creativecommons.org/licenses/by-nc-nd/4.0/>.



**Publisher's statement:**

Please refer to the repository item page, publisher's statement section, for further information.

For more information, please contact the WRAP Team at: [wrap@warwick.ac.uk](mailto:wrap@warwick.ac.uk).

# Flexural buckling behaviour and design of duplex and ferritic stainless steel I-section columns

Merih Kucukler

*School of Engineering, University of Warwick, Coventry, CV4 7AL, UK*

---

## Abstract

In this paper, the flexural buckling behaviour and design of duplex and ferritic stainless steel I-section columns fabricated through the welding of individual hot-rolled stainless steel plates are investigated. Finite element models able to mimic the structural response of stainless steel I-section columns are developed and validated against experimental results from the literature. Employing the validated finite element models, extensive numerical parametric studies are performed for the purpose of comprehensively assessing the behaviour of duplex and ferritic stainless steel I-section columns, considering various member slendernesses and cross-section proportions. The accuracy, safety and applicability of the existing column design provisions provided in the European, North American and Australian & New Zealand structural stainless steel design standards and guides, some of which are only recommended for the design of cold-formed stainless steel columns, are assessed for the design of welded duplex and ferritic stainless steel I-section columns. Modifications to the column design method given in the current European structural stainless steel design standard EN 1993-1-4 are proposed. The higher accuracy of the modified column design method of EN 1993-1-4 relative to the column design methods in the existing structural stainless steel design standards and guides is illustrated in addition to its safety and high level of reliability.

*Keywords:* Buckling, Columns, Duplex stainless steel, Experiments, Ferritic stainless steel, Flexural buckling, I-section, Instability, Numerical modelling, Stainless steel

---

## 1. Introduction

Owing to its unique combination of excellent corrosion resistance, durability, attractive appearance and favourable mechanical properties, stainless steel is increasingly being used in the construction industry. Thus far, cold-formed hollow section stainless steel structural elements have been the primary product types employed in construction; the behaviour of such members has been investigated extensively in the literature [1–8] with the development of design guidance that featured in design standards [9–12]. However, increasing demands

---

*Email address:* merih.kucukler@warwick.ac.uk (Merih Kucukler)

for higher structural resistances for stainless steel members rendered the requirement of the use of larger and typically welded I-section stainless steel members in construction. This generated a need for research focusing on the structural response of welded stainless steel I-section members and the development of design guidance providing accurate and safe estimations of their behaviour.

Recognising the necessity of research into the behaviour of welded stainless steel I-section members, experimental and numerical studies focusing on their structural response have recently been performed in the literature. Yang et al. [13, 14], Burgan et al. [15], Zheng et al. [16] and Ahmed et al. [17] carried out experiments on arc-welded austenitic and duplex stainless steel I-section columns and beam-columns. Yuan et al. [18] proposed residual stress patterns for arc-welded austenitic, duplex and ferritic stainless steel I-sections on the basis of data obtained from a series of residual stress measurements. In Bredenkamp and Van den Berg [19], a series of arc-welded ferritic stainless steel I-section columns were tested. Yang et al. [20] and Wang et al. [21] performed experiments on laterally-unrestrained welded austenitic stainless steel I-section beams. Gardner et al. [22] initiated a research programme focusing on the investigation of the structural response of laser-welded austenitic stainless steel I-section members, conducting residual stress measurements, stub column tests, column flexural buckling tests, bending tests on laterally-restrained beams [23] and experiments on laterally-restrained beam-columns [24]. Bu and Gardner [25] analysed the accuracy of the existing design methods for arc-welded and laser-welded austenitic stainless steel I-section columns. Saliba and Gardner [26] and Yuan et al. [27] investigated the cross-section response of lean duplex stainless steel I-section structural elements. Yuan et al. [28] tested austenitic and duplex stainless steel I-section columns subjected to interactive local and global buckling. Finally, Kucukler et al. [29] carried out a series of experiments on laterally-unrestrained laser-welded austenitic stainless steel I-section beam-columns and developed design guidance for their flexural-torsional buckling assessment. Even though there is a significant increase in the research studies investigating the structural response of stainless steel I-section members recently, the previous research has primarily focused on the behaviour of austenitic stainless steel I-section structural elements, the structural response of duplex and ferritic stainless steel I-section members has not been comprehensively investigated, the accuracy of the existing design rules for such members has not been extensively assessed and a complete design guidance providing accurate estimations of their response under various loading conditions has not been yet established.

With the aim of initiating a comprehensive investigation into the behaviour and design of welded duplex and ferritic stainless steel I-section members, a research study focusing on the flexural buckling response and design of duplex and ferritic stainless steel I-section columns fabricated through the welding of individual hot-rolled stainless steel plates is performed in this paper. Finite element models able to replicate the structural response of welded duplex and ferritic stainless steel I-section columns are created and validated against experimental results from the literature. Using the validated finite element models, extensive numerical parametric studies are carried out. The accuracy of the existing design methods for the design of duplex and ferritic stainless steel columns is investigated. Modifications to the column design method provided in the European structural stainless steel design standard

EN 1993-1-4 [9] are proposed. The higher accuracy of the modified EN 1993-1-4 [9] column design method relative to the existing column design methods provided in the structural stainless steel design standards and guides [9–12] is shown for duplex and ferritic stainless steel I-section columns in addition to its safety and high level of reliability.

## 2. Finite element modelling

The details of the finite element modelling approach adopted in this study and its validation against experimental results from the literature are provided in this section. In the following sections, structural performance data obtained through the Geometrically and Materially Nonlinear Analyses with Imperfections (GMNIA) of the finite element models are utilised to (i) assess the accuracy of the existing design guidance for duplex and ferritic stainless steel I-section columns and (ii) modify the column design method provided in EN 1993-1-4 [9] to achieve more accurate estimations of the structural response of duplex and ferritic stainless steel I-section members under pure axial compression.

### 2.1. Element type and modelling assumptions

In this study, the finite element models were created using the finite element analysis software Abaqus [30]. The four-noded reduced integration general purpose shell finite element S4R [30], which has been successfully adopted for similar applications [29, 31–34], was used to create all the finite element models. To capture the spread of plasticity through the depth of the cross-section accurately, 16 elements were used to model the flanges and web of an I-section. To avoid the overlapping of the flange and web plates, the web plate was offset taking into account the thickness of flanges. The number of the finite elements along the lengths were selected such that the aspect ratios of the elements were approximately equal to unity. The default Simpson integration method was used, with five integration points through the thickness of each element. The Poisson’s ratio was taken as 0.3 in the elastic range and 0.5 in the plastic range by defining the effective Poisson’s ratio as 0.5 to allow for the change of cross-sectional area under load. The von Mises yield criterion with the associated flow rule and isotropic strain hardening were assumed in the models. To represent the engineering stress-strain ( $\sigma - \epsilon$ ) response of stainless steel, the two stage compound Ramberg-Osgood material model, illustrated in Fig. 1 (a), was used as given by eqs. (1) and (2):

$$\epsilon = \frac{\sigma}{E} + 0.002 \left( \frac{\sigma}{f_y} \right)^n \quad \text{for } \sigma \leq f_y, \quad (1)$$

$$\epsilon = \frac{\sigma - f_y}{E_{p0.2}} + \left( \epsilon_u - \epsilon_{p0.2} - \frac{f_u - f_y}{E_{p0.2}} \right) \left( \frac{\sigma - f_y}{f_u - f_y} \right)^m + \epsilon_{p0.2} \quad \text{for } f_y < \sigma \leq f_u, \quad (2)$$

where  $n$  and  $m$  are strain hardening exponents,  $f_y$  is the yield stress taken as the 0.2% proof stress,  $E$  is the Young’s modulus,  $E_{p0.2}$  and  $\epsilon_{p0.2}$  are the tangent modulus and total strain corresponding to the 0.2% proof stress  $f_y$  respectively, and  $f_u$  and  $\epsilon_u$  are the ultimate tensile strength and strain. In this study, the standardised material properties for hot-rolled

duplex and ferritic stainless steel plates put forward by [35] on the basis of a high number of measurements of material properties of such plates collected from the literature were utilised to define the material properties of duplex and ferritic I-section columns. The use of these values was recommended for welded stainless steel I-sections in [35], which are typically fabricated by the welding of individual hot-rolled stainless steel plates. The standardised values of  $f_y$ ,  $f_u$ ,  $\epsilon_u$ ,  $n$  and  $m$  for hot-rolled duplex and ferritic stainless steel plates used in this study are provided in Table 1. The engineering stress-strain response adopted in the finite element models of duplex and ferritic stainless steel columns is shown in Fig. 1 (b). Since the constitutive formulations of Abaqus [30] adopt the Cauchy (true) stress-strain assumption for the adopted element type, the engineering stress-strain response shown in Fig. 1 (b) was transformed into the true stress-log plastic strain ( $\sigma_{true}-\epsilon_{true}^{pl}$ ) and input into Abaqus [30], defining true stress  $\sigma_{true}$  values as

$$\sigma_{true} = \sigma (1 + \epsilon), \quad (3)$$

and calculating log plastic strain  $\epsilon_{true}^{pl}$  values as

$$\epsilon_{true}^{pl} = \ln(1 + \epsilon) - \frac{\sigma_{true}}{E}. \quad (4)$$

In the finite element models, pin-end support conditions were established using kinematic coupling constraints. The nodes within the end sections were constrained to a reference point located at the centroid of the cross-section where the boundary conditions were defined.

## 2.2. Geometric imperfections

Both local and global geometric imperfections were applied to the finite element models of columns by using their lowest local and global buckling modes obtained from their Linear Eigenvalue Analyses (LEA) as shown in Fig. 2. For the case of local imperfections, the lowest local buckling modes were scaled to local imperfection magnitudes  $\omega_{local}$  determined on the basis of the modified Dawson and Walker model [36, 37] as given by

$$\omega_{local} = 0.023 \left( \frac{f_y}{f_{cr,min}} \right) t \quad (5)$$

and applied to the finite element models; the Dawson and Walker model was also adopted to define local imperfections in stainless steel I-section members in [23–26, 38] where its appropriateness was verified. In eq. (5),  $f_{cr,min}$  is the minimum elastic buckling stress of all the plates constituting the section and  $t$  is the thickness of the plate element. Global imperfections were applied to the finite element models by using the lowest global buckling modes and taking the highest global geometric imperfection magnitude  $\omega_{global}$  as 1/1000 of the column lengths  $L$ , i.e.  $\omega_{global} = L/1000$ . It should be noted that the global buckling modes used to apply the global geometric imperfections to the finite element models were obtained through Linear Eigenvalue Analyses (LEA) where all the nodes within the flange and web plates were constrained to the centroids of the corresponding plates, thereby suppressing local buckling modes. Moreover, the local buckling modes used in the application of the local geometric imperfections to the finite element models were obtained by carrying out LEA where the translations of the columns about the principal buckling axes were restrained at the web-flange junctions along their lengths.

### 2.3. Residual stresses

The residual stress pattern put forward by Yuan et al. [18] and shown in Fig. 3, based on a series of measurements made on welded duplex and ferritic stainless steel I-section members, was used to define residual stresses in the finite element models in this paper. As can be seen in Fig. 3, the maximum tensile residual stresses within the flanges  $\sigma_{ft}$  and webs  $\sigma_{wt}$  are taken as 60% of the 0.2% proof stress  $f_y$  (i.e.  $\sigma_{ft} = \sigma_{wt} = 0.6f_y$ ). The maximum compressive residual stresses within the flanges  $\sigma_{fc}$  and webs  $\sigma_{wc}$  were determined on the basis of the axial force equilibrium in accordance with the recommendations of [18]. The residual stress pattern displayed in Fig. 3 was included in the finite element models in a step-wise fashion by defining constant values (taken at the middle of each element) of residual stress at the element integration points. The residual stresses were applied to the finite element models within a separate step finalised with the achievement of the equilibrium prior to the application of the loading. Since stainless steel has nonlinear material stress-strain response, the implementation of residual stresses to the finite element models results in permanent strains; thus, the residual plastic strains  $\epsilon_{res,pl}$  corresponding to the assigned residual stresses  $\sigma_{res}$  were also applied to the finite element models. Considering the two-stage compound Ramberg-Osgood material model, the following expression was utilised to define the residual plastic strains  $\epsilon_{res,pl}$  at the cross-section integration points of the finite element models [39]:

$$\epsilon_{res,pl} = 0.002 \left( \frac{\sigma_{res}}{f_y} \right)^n, \quad (6)$$

where  $\sigma_{res}$  is the corresponding residual stress applied at the cross-section integration point. The implementation of the residual plastic strains  $\epsilon_{res,pl}$  is necessary to ensure that the residual stress pattern illustrated in Fig. 3 is achieved after the equilibrium load step.

### 2.4. Validation of numerical models

In this subsection, the finite element modelling approach adopted in this study is validated against the results obtained from experiments carried out by Burgan et al. [15] and Yang et al. [13] on arc-welded duplex stainless steel I-section columns and by Bredenkamp and Van den Berg [19] on arc-welded ferritic stainless steel I-section columns.

#### 2.4.1. Validation against experiments performed by Burgan et al. [15] and Yang et al. [13] on arc-welded duplex stainless steel I-section columns

Validation of the finite element modelling approach against the experiments performed by Burgan et al. [15] and Yang et al. [13] on arc-welded duplex stainless steel I-section columns is provided in this section. In Burgan et al. [15], three grade 1.4462 duplex stainless steel I-section columns subjected to major axis buckling with different buckling lengths  $L_{cr}$  were tested. The specimens, which had pin-end support conditions, had the cross-section shape designated herein as I160×160×6×8 adopting the following designation system: I - section height ( $h$ ) × flange width ( $b$ ) × web thickness ( $t_w$ ) × flange thickness ( $t_f$ ). In Yang et al. [13], eleven grade 1.4462 (2205) duplex stainless steel columns with different buckling

lengths  $L_{cr}$  were tested, five of which were subjected to major axis buckling and six of which were subjected to minor axis buckling. Nine of the column specimens tested by Yang et al. [13] had a I150×150×6×10 cross-section, while the remaining two had I110×150×6×10 and I150×120×6×10 sections. In the experiments of [13], a pair of knife edges were used to establish pin-end support conditions; the buckling lengths of the specimens were equal to the specimen lengths plus the total lengths of the knife edges at the both ends (i.e.  $L_{cr} = L + 340$  mm). As described in Section 2.1, in the finite element models created in this study, the nodes within the end sections were constrained to a reference point located at the centroid of the cross-section by means of coupling constraints where the boundary conditions were applied; in the case of the finite element models of the specimens tested by Yang et al. [13], the reference points were longitudinally offset from each end by 170 mm to represent the distance between the end of the specimen and the tip of the knife edge. The material properties of the specimens reported in [13, 15] were adopted in the finite element models, using the two-stage Ramberg-Osgood material model given by eqs. (1) and (2) with the strain hardening exponents provided in Table 1 for duplex stainless steel. The geometric imperfections and residual stresses were applied to the models as described in Section 2.2

The ultimate strengths of the specimens obtained in the experiments of Burgan et al. [15] and Yang et al. [13]  $N_{ult,test}$  are compared against those determined through the finite element modelling approach adopted in this study  $N_{ult,FE}$  in Table 2. As can be seen from the table, the finite element models provide flexural buckling strengths  $N_{ult,FE}$  in a good agreement with those observed during the experiments  $N_{ult,test}$  for both major and minor axis buckling and different buckling lengths, indicating that the finite element modelling approach adopted in this study is able to replicate the structural response of stainless steel I-section columns. In Fig. 4 and Fig. 5, the axial compression versus axial deformation and the axial compression versus mid-height lateral deformation paths observed in the experiments of Yang et al. [13] and those obtained from the finite element models created in this study are compared for the specimens subjected to major and minor axis buckling, respectively. As can be seen from Fig. 4 and Fig. 5, the agreement between the experimentally and numerically obtained load versus deformation paths is very good, indicating that the finite element models created in this study are able to mimic the behaviour of stainless steel I-section columns. The failure mode of the I2205-2000 specimen observed during the experiment of [13] and that obtained through its finite element model created herein are shown in Fig. 6, where it can be seen that the finite element model of the specimen provides a failure mode in accordance with that observed during the experiment.

#### *2.4.2. Validation against experiments performed by Bredenkamp and Van den Berg [19] on arc-welded ferritic stainless steel I-section columns*

In this subsection, the finite element modelling approach adopted in this study is validated against the experiments performed by Bredenkamp and Van den Berg [19] on fifteen arc-welded grade 1.4003 (3CR12) ferritic stainless steel I-section columns, which is the only experimental study on welded ferritic stainless steel I-section columns found in the literature. Nine columns had the cross-section shape of I140×70×3.5×5.5 and six columns had the cross-section shape of I180×90×4.5×6, which were fabricated through the welding of

individual 1.4003 ferritic stainless steel plates. The specimens, which were subjected to minor axis buckling, had pin-ended support conditions. In the finite element models created herein, the corresponding material properties obtained through the tests performed on stub columns with I140×70×3.5×5.5 and I180×90×4.5×6 sections reported by [19] were used for the columns made of these sections, using the two-stage Ramberg-Osgood material model given by eqs. (1) and (2) with the strain hardening exponents provided in Table 1 for ferritic stainless steel. Note that the specimens underwent plastic deformations during their fabrication carried out by [19] as reported in [19], which led to the enhancements of the 0.2% proof strengths  $f_y$  of the virgin plates used in their fabrication. The geometric imperfections and residual stresses were applied to the models as described in Section 2.2. In Fig. 7, the ultimate strengths of the columns obtained from the experiments and those determined using the finite element models created herein are compared, where  $A$  is the cross-section area of the column and  $\bar{\lambda}_z$  is the non-dimensional minor axis flexural buckling slenderness determined by taking the square root of the ratio of the cross-section 0.2% proof strength resistance (i.e.  $Af_y$ ) to minor axis elastic critical buckling load  $N_{cr,z}$ , (i.e.  $\bar{\lambda}_z = \sqrt{Af_y/N_{cr,z}}$ ). Fig. 7 shows that the ultimate resistances determined by the finite element models and those obtained from the experiments generally follow the same trend, reducing with the increasing non-dimensional slenderness  $\bar{\lambda}_z$ . For seven out of fifteen columns, the ratios of the ultimate resistances observed in the experiments to those determined through the finite element models created herein were greater than 1.30 though. These differences were ascribed to the differences in the shapes and magnitudes of the geometric imperfections assumed in the finite element models and those present in the specimens, which were not reported by [19], and the differences in the material properties used in the finite element models which were obtained from the two stub column tests performed by [19] and those of the specimens which may have undergone different extents of work hardening during their fabrication performed by [19]. Moreover, as can be seen in Fig. 7, the ultimate resistances of some slender specimens observed in the experiments of [19] are greater than their Euler critical buckling loads; this response is somewhat questionable and signifies that other than those reported in [19], there could be an additional support afforded to the specimens during the experiments which may be due to frictions at the end supports. Since (i) the ratios between the experimentally and numerically determined ultimate resistances are less than or equal to 1.30 for eight out of fifteen specimens, (ii) the finite element models invariably provide conservative estimations of the column resistances and (iii) the finite element models were extensively validated in the previous subsection for duplex stainless steel I-section columns in which only the material properties are changed herein, it was assumed that the finite element models provide appropriate and safe ultimate strength predictions for ferritic stainless steel I-section columns. It should also be noted that the finite element modelling approach adopted in this study has also been extensively validated in Kucukler et al. [29].

### 3. Parametric studies

For the purpose of comprehensively investigating the structural response of welded duplex and ferritic stainless steel I-section columns, extensive numerical parametric studies were



carried out in this paper. A summary of the considered parameters is provided in Table 3. In the parametric studies, a constant cross-section depth  $h$  equal to 150 mm (i.e.  $h = 150$  mm) was adopted, whereas four different flange widths were taken into consideration, resulting in four cross-section aspect ratios  $h/b$  equal to 1.0, 1.5, 2.0 and 3.0 (i.e.  $h/b = 1.0, 2.0, 3.0$  and 4.0). Three different values of flange thickness  $t_f$  and web thickness  $t_w$  were chosen for each cross-section aspect ratio to generate a spectrum of local slenderness covering sections ranging from Class 1 to Class 3 in accordance with the slenderness limits provided in EN 1993-1-4 [9]. The web and flange thicknesses were chosen such that the web plate slenderness  $\bar{\lambda}_{p,w}$  and the flange plate slenderness  $\bar{\lambda}_{p,f}$  of the modelled cross-sections were virtually the same; the web and flange plate slendernesses were determined from eqs. (7) and (8):

$$\bar{\lambda}_{p,w} = \sqrt{f_y/f_{cr,w}}, \quad (7)$$

$$\bar{\lambda}_{p,f} = \sqrt{f_y/f_{cr,f}}, \quad (8)$$

where  $f_{cr,w}$  and  $f_{cr,f}$  are the elastic buckling stresses of the web and flange plates considered in isolation, respectively. Columns with 10 different length  $L$  to cross-section depth  $h$  ratios  $L/h$  were modelled for each considered cross-section which were subjected to both major and minor axis buckling;  $L/h$  ratios were taken such that the non-dimensional flexural buckling slendernesses of the columns about the considered buckling axis ( $\bar{\lambda}_z, \bar{\lambda}_y$ ) varied between 0.1 and 2.5. Note that the non-dimensional major and minor axis flexural buckling slendernesses are determined by taking the square root of the ratio of the cross-section 0.2% proof strength  $Af_y$  to the major axis  $N_{cr,y}$  and minor axis  $N_{cr,z}$  elastic critical buckling loads respectively (i.e.  $\bar{\lambda}_y = \sqrt{Af_y/N_{cr,y}}$  and  $\bar{\lambda}_z = \sqrt{Af_y/N_{cr,z}}$ ).

In the following subsections, a series of findings of the extensive numerical parametric studies performed in this paper are summarised, while the results obtained from the parametric studies are used in the following sections to assess the accuracy of the existing design methods for duplex and ferritic stainless steel I-section columns and improvement of EN 1993-1-4 [9] column design method for more accurate assessment of their behaviour.

### 3.1. Influence of stainless steel grade

Fig. 8 shows the influence of the steel grade on the major axis and minor axis flexural buckling resistances of welded duplex and ferritic stainless steel columns for (i) different major axis  $\bar{\lambda}_y$  and minor axis  $\bar{\lambda}_z$  non-dimensional slenderness values and (ii) for columns with all the considered sections and for those with Class 3 I150×150×4.95×8.24 and I150×150×3.92×6.41 sections. In Fig. 8, the axial compression resistances are normalised by cross-section 0.2% proof strengths (i.e.  $N_{Ed}/Af_y$ ). As can be seen from the figure, the steel grade influences the normalised axial compression resistances  $N_{Ed}/Af_y$  of columns with non-dimensional slenderness values less than or equal to 0.6 (i.e.  $\bar{\lambda}_y \leq 0.6$  and  $\bar{\lambda}_z \leq 0.6$ ), where duplex stainless steel columns have greater normalised resistances  $N_{Ed}/Af_y$  relative to those of ferritic stainless steel columns. For columns with higher non-dimensional slendernesses (i.e.  $\bar{\lambda}_y > 0.6$  and  $\bar{\lambda}_z > 0.6$ ), the influence of the steel grade on the normalised axial compression resistances  $N_{Ed}/Af_y$  becomes quite small.

### 3.2. Influence of axis of buckling

In Fig. 9, the influence of the axis of buckling on the normalised compression resistances of duplex and ferritic stainless steel columns is shown for different non-dimensional flexural buckling slendernesses  $\bar{\lambda}$  and for major axis buckling and minor axis buckling. Note that in Fig. 9,  $\bar{\lambda}$  is equal to the non-dimensional major  $\bar{\lambda}_y$  and minor axis  $\bar{\lambda}_z$  buckling slenderness of columns undergoing major and minor axis buckling, respectively. As can be seen from the figure, the axis of buckling significantly affects the normalised strengths of the duplex and ferritic stainless steel columns, where the normalised ultimate resistances of the columns  $N_{Ed}/Af_y$  are lower for the case of minor axis buckling. This results from the more rapid erosion of the minor axis flexural stiffness of the columns  $EI_z$  relative to the erosion rate of their major axis flexural stiffnesses  $EI_y$  due to the presence of the residual stresses as shown in Fig. 3.

### 3.3. Influence of cross-section aspect ratio

Fig. 10 illustrates the influence of the cross-section aspect ratios on the normalised axial compression resistances  $N_{Ed}/Af_y$  of duplex and ferritic stainless steel I-section columns for cross-section aspect ratios  $h/b$  of 1.0, 1.5, 2.0 and 3.0 (i.e.  $h/b = 1.0, 2.0, 3.0$ ), different axis of buckling and non-dimensional slendernesses. As can be seen from Fig. 10, the cross-section aspect ratio of the columns is more important for duplex and ferritic stainless steel I-section columns undergoing major axis buckling relative to those experiencing minor axis buckling. However, for both major axis and minor axis flexural buckling, the influence of the cross-section aspect ratio of a column on the normalised resistances  $N_{Ed}/Af_y$  is rather small, indicating that an adjustment to flexural buckling design curves is not necessary for columns with different cross-section shapes unlike for lateral-torsional buckling design curves used for steel beams as shown in [29, 31, 33]. Note that in addition to the influence of the stainless steel grade, the axis of buckling and the cross-section aspect ratio, the influence of the class of a column cross-section on its normalised resistance  $N_{Ed}/Af_y$  was also investigated; it was observed that the cross-section class becomes influential only for the normalised strengths  $N_{Ed}/Af_y$  of very stocky columns with  $\bar{\lambda}_y \leq 0.2$  and  $\bar{\lambda}_z \leq 0.2$ , for which local instability effects are of importance for the ultimate resistances.

## 4. Assessment of existing design rules for stainless steel I-section columns

### 4.1. Introduction

In this section, the accuracy of the European EN 1993-1-4 [9], North American ASCE/SEI-8 [10] and Australian & New Zealandian AS/NSZ 4673:2001 [11] stainless steel design standards is assessed for the design of welded duplex and ferritic stainless steel I-section columns. Additionally, the accuracy of the American Institute of Steel Construction (AISC) Design Guide 27 [12] for stainless steel structures is also assessed. It should be emphasised that unlike EN 1993-1-4 [9] and AISC Design Guide 27 [12], the design methods provided in ASCE/SEI-8 [10] and AS/NSZ 4673:2001 [11] are only applicable to cold-formed stainless steel members. However, it is still found worthwhile to assess their accuracy in this study so as to identify whether they are also applicable to duplex and ferritic stainless steel I-section columns fabricated through the welding of individual hot-rolled stainless steel plates.

#### 4.2. European structural stainless steel design standard EN 1993-1-4 [9]

In accordance with the carbon steel design standard EN 1993-1-1 [40], EN 1993-1-4 [9] adopts the Perry-Robertson concept [41, 42] for the estimation of the ultimate resistances of stainless steel I-section columns. According to EN 1993-1-4 [9], the design buckling resistance of a stainless steel I-section column  $N_{b,Rd}^{EC3}$  is determined as

$$\begin{aligned} N_{b,Rd}^{EC3} &= \frac{\chi A f_y}{\gamma_{M1}} \quad \text{for Class 1, 2 and 3 sections,} \\ N_{b,Rd}^{EC3} &= \frac{\chi A_{eff} f_y}{\gamma_{M1}} \quad \text{for Class 4 sections,} \end{aligned} \quad (9)$$

where  $A_{eff}$  is the effective cross-section area for a Class 4 section determined in accordance with the effective width rules provided in [9],  $\gamma_{M1}$  is the partial safety factor taken as 1.1 (i.e.  $\gamma_{M1} = 1.1$ ) and  $f_y$  is the yield stress taken as the 0.2% proof strength. In eq. (9),  $\chi$  is the buckling reduction factor calculated as:

$$\begin{aligned} \chi &= \frac{1}{\phi + \sqrt{\phi^2 - \bar{\lambda}^2}} \\ \text{where } \phi &= 0.5 \left[ 1 + \eta + \bar{\lambda}^2 \right] \end{aligned} \quad (10)$$

in which  $\eta$  is the generalised imperfection factor determined using the following expression:

$$\eta = \alpha (\bar{\lambda} - \bar{\lambda}_0) \quad (11)$$

where  $\alpha$  is the imperfection factor and  $\bar{\lambda}_0$  is the threshold slenderness; for columns with  $\bar{\lambda} \leq \bar{\lambda}_0$ , the buckling reduction factor  $\chi$  is equal to unity (i.e.  $\chi = 1.0$ ). For welded stainless steel I-section columns, EN 1993-1-4 [9] recommends the use of imperfection factor  $\alpha$  and threshold slenderness  $\bar{\lambda}_0$  values given in Table 4.

#### 4.3. AISC Design Guide 27 [12]

AISC Design Guide 27 [12] recommends the following expression for the determination of the design buckling resistance of a stainless steel column  $N_{b,Rd}^{AISC}$  undergoing flexural buckling:

$$N_{b,Rd}^{AISC} = \phi_c P_n = \phi_c F_{cr} A_g \quad (12)$$

where  $P_n$  is the compression resistance value determined considering flexural buckling,  $\phi_c$  is the resistance factor taken as 0.9 (i.e.  $\phi_c = 0.9$ ),  $F_{cr}$  is the buckling stress and  $A_g$  is the cross-section area of the stainless steel column. Adopting the EN 1993-1-4 [9] format, the buckling stress of a stainless steel column  $F_{cr}$  according to AISC Design Guide 27 [12] can be expressed as

$$F_{cr} = \chi f_y, \quad (13)$$

in which  $\chi$  can be calculated as follows:

$$\chi = Q \left( 0.50 Q \bar{\lambda}^2 \right) \quad \text{for } \bar{\lambda} \leq 1.20$$

$$\chi = \frac{0.531}{\bar{\lambda}^2} \quad \text{for } \bar{\lambda} > 1.20, \quad (14)$$

where  $Q$  is the reduction factor for local buckling which is taken as equal to 1.0 for non-slender cross-section.

#### 4.4. North American structural stainless steel design standard ASCE/SEI-8 [10]

In ASCE/SEI-8 [10], the adoption of the tangent modulus theory of buckling is recommended for the determination of the design buckling resistance of stainless steel columns. According to ASCE/SEI-8 [10], the design buckling resistance of a stainless steel column  $N_{b,Rd}^{ASCE/SEI}$  for flexural buckling is determined as

$$N_{b,Rd}^{ASCE/SEI} = \phi_c f_n A_e \quad (15)$$

where  $\phi_c$  is the resistance factor taken as 0.85 (i.e.  $\phi_c = 0.85$ ) and  $f_n$  is the flexural buckling stress calculated as

$$f_n = \frac{\pi^2 E_t}{(KL/r)^2} \quad (16)$$

in which  $K$  is the effective length factor,  $L$  is the unbraced length of the member,  $r$  is the radius of gyration of full section and  $E_t$  is the tangent modulus in compression corresponding to the buckling stress which is taken as

$$E_t = \frac{f_y E}{f_y + 0.002nE(f_n/f_y)^n}, \quad (17)$$

where  $n$  is the Ramberg-Osgood exponent for the initial part of the stress-strain curve as described in Section 2.1. Since the tangent modulus  $E_t$  is a function of applied axial compression as can be seen from eqs. (15), (16) and (17), ASCE/SEI-8 [10] requires iteration for the determination of the flexural buckling resistances of stainless steel columns.

#### 4.5. Australian & New Zealandian structural stainless steel design standard AS/NSZ 4673:2001 [11]

The Australian & New Zealandian AS/NSZ 4673:2001 [11] standard sets out two design methods for the estimations of the flexural buckling resistances of stainless steel columns: (i) the iterative tangent modulus theory of buckling approach as adopted in ASCE/SEI-8 [10] with the same resistance factor value equal to 0.85 (i.e.  $\phi_c = 0.85$ ) and (ii) a design method based on the Perry-Robertson concept similar to EN 1993-1-4 [9]. According to the latter, the design buckling resistance of a column  $N_{b,Rd}^{AS/NSZ}$  is calculated as

$$N_{b,Rd}^{AS/NSZ} = \phi_c f_n A_e \quad (18)$$

where  $\phi_c$  is the resistance factor taken as 0.90 (i.e.  $\phi_c = 0.90$ ) and  $f_n$  is the flexural buckling stress calculated as

$$f_n = \frac{f_y}{\phi + \sqrt{\phi^2 - \bar{\lambda}^2}} \leq f_y$$

$$\text{where } \phi = 0.5 \left( 1 + \eta + \bar{\lambda}^2 \right). \quad (19)$$

The generalised imperfection factor  $\eta$  is determined using the following expression:

$$\eta = \alpha \left[ (\bar{\lambda} - \lambda_1)^\beta - \lambda_0 \right] \quad \text{with} \quad \bar{\lambda} = \frac{KL}{r} \sqrt{\frac{f_y}{\pi^2 E_0}} \quad (20)$$

The parameters  $\alpha$ ,  $\beta$ ,  $\lambda_0$ ,  $\lambda_1$  and  $E_0$  used in eq. (20) are provided in Table 5 for duplex and ferritic stainless steel columns. Note that in the following subsection, the accuracy of AS/NSZ 4673:2001 [11] for the ultimate resistance predictions of duplex and ferritic stainless steel columns will be assessed considering the design method based on the Perry-Robertson concept described above. The accuracy of the column design method based on the tangent modulus theory of buckling given in AS/NSZ 4673:2001 [11] is the same as that of the column design method provided in ASCE/SEI-8 [10] as both methods are identical.

#### 4.6. Assessment of the accuracy of the existing design methods for welded duplex and ferritic stainless steel I-section columns

In this subsection, the accuracy of the existing design methods for the flexural buckling strength predictions of welded duplex and ferritic stainless steel I-section columns is investigated. Note that since safety factors were not applied to the material strength and stiffness in the finite element simulations, the safety factors were taken as equal to 1.0 in the predictions of the ultimate column resistances on the basis of all the existing design methods described in the previous subsections herein in accordance with [43–45] (i.e.  $\gamma_{M1} = 1.0$ ,  $\phi_c = 1.0$ ). Fig. 11 shows the accuracy of EN 1993-1-4 [9] and AISC Design Guide 27 [12] with respect to the the ultimate strength predictions of welded duplex and ferritic stainless steel I-section columns for different axes of buckling, non-dimensional slenderness  $\bar{\lambda}_y, \bar{\lambda}_z$  values, different cross-section aspect ratios and cross-section classes shown in Table 3, using the numerical results obtained from the GMNIA of the finite element models and the experimental results collected from [13, 15, 19]. As can be seen from Fig. 11, AISC Design Guide 27 [12] generally provides overly-conservative flexural buckling strength predictions for welded I-section stainless steel columns; AISC Design Guide 27 [12] is particularly very overly-conservative for slender columns. Even though EN 1993-1-4 [9] leads to more accurate ultimate resistance predictions relative to AISC Design Guide 27 [12], Fig. 11 suggests that there is still room for improvement in its accuracy as the flexural buckling strength predictions obtained from EN 1993-1-4 [9] are overly-conservative for some cases.

In addition to the accuracy of EN 1993-1-4 [9] and AISC Design Guide 27 [12], the accuracy of the North American structural stainless steel design standard ASCE/SEI-8 [10] and Australian & New Zealandian structural stainless steel design standard AS/NSZ

4673:2001 [11] is also assessed in Fig. 12 for welded I-section duplex and ferritic stainless steel columns, where  $R_{method}$ ,  $R_{GMNIA}$  and  $R_{experiment}$  are the ultimate resistance predictions obtained from a design method, GMNIA and experiment respectively,  $\epsilon$  is the parameter for the assessment of the accuracy of a design method equal to the ratio of the ultimate strength prediction obtained from a GMNIA or experiment to that determined through a design method (i.e.  $\epsilon = R_{GMNIA}/R_{method}$  or  $\epsilon = R_{experiment}/R_{method}$ ) and  $\bar{\lambda}$  is equal to the major axis  $\bar{\lambda}_y$  and minor axis  $\bar{\lambda}_z$  flexural buckling non-dimensional slendernesses for major and minor axis flexural buckling, respectively. As can be seen from Fig. 12, both ASCE/SEI-8 [10] and AS/NSZ 4673:2001 [11] lead to quite unsafe ultimate strength predictions for duplex and ferritic stainless steel I-section columns. The level of unsafety is higher for the case of ASCE/SEI-8 [10]. The unsafe results obtained using ASCE/SEI-8 [10] and AS/NSZ 4673:2001 [11] result from the fact that the column design methods of these standards were originally developed for cold-formed stainless steel columns; the results provided in Fig. 12 indicate that the column design methods of [10, 11] may not be applicable to duplex and ferritic stainless steel I-section columns fabricated through the welding of individual hot-rolled stainless steel plates. Since the residual stresses shown in Fig. 3 resulting from the welding of individual plates may lead to considerable reductions in the ultimate strengths, the column design methods of these standards originally developed for cold-formed steel columns, in which membrane residual stresses are small and work hardening in the corner regions can significantly contribute to the ultimate strengths, lead to unsafe results for welded duplex and ferritic stainless steel I-section columns.

A statistical appraisal of the accuracy of EN 1993-1-4 [9], AISC Design Guide 27 [12], ASCE/SEI-8 [10] and AS/NSZ 4673:2001 [11] for the flexural buckling strength predictions of welded duplex and ferritic stainless steel I-section columns is provided in Table 6, considering all the parameters shown in Table 3 in the GMNIA simulations and using the experimental results obtained from [13, 15, 19]. In Table 6,  $N$  is the number of considered columns,  $\epsilon$  is equal to the ratio of the ultimate resistance prediction obtained from a GMNIA or experiment to that determined through a design method (i.e.  $\epsilon = R_{GMNIA}/R_{method}$  or  $\epsilon = R_{experiment}/R_{method}$ ) and  $\epsilon_{av}$ ,  $\epsilon_{COV}$ ,  $\epsilon_{max}$  and  $\epsilon_{min}$  are the average, coefficient of variation, maximum and minimum of the  $\epsilon$  values. Table 6 shows that amongst the existing structural stainless steel design standards and guides, EN 1993-1-4 [9] leads to the most accurate flexural buckling strength predictions for welded duplex and ferritic stainless steel I-section columns. However, in some cases, EN 1993-1-4 [9] still leads to overly-conservative ultimate strength predictions, signifying the scope for improvement in the accuracy of the column design method of EN 1993-1-4 [9] for duplex and ferritic stainless steel I-section columns.

It should be noted that in [25], it was observed that the column design method of EN 1993-1-4 [9] generally leads to accurate but sometimes conservative results for austenitic stainless steel I-section columns. Considering that residual stresses within duplex and ferritic stainless steel I-sections are lower than those within austenitic stainless I-sections determined on the basis of experimental measurements [18], it is expected that the column design method of EN 1993-1-4 [9] can lead to accurate results for austenitic stainless steel I-section columns but overly-conservative strength predictions for duplex and ferritic stainless steel I-section columns since EN 1993-1-4 [9] does not provide different buckling curves with different

imperfection factors  $\alpha$  for austenitic, duplex and ferritic stainless steel I-section columns unlike AS/NSZ 4673:2001 [11].

In line with the observations made in Fig. 11, Table 6 also shows that the AISC Design Guide 27 [12] provides very overly-conservative and inaccurate ultimate strength predictions for duplex and ferritic I-section welded columns, thus leading to very uneconomic designs which is particularly undesirable considering that stainless steel is an expensive construction material. In Table 6, the unsafety of ASCE/SEI-8 [10] and AS/NSZ 4673:2001 [11] can be observed for welded duplex and ferritic stainless steel I-section columns, signifying that the column design methods of these standards cannot be applied to such members. Note that ASCE/SEI-8 [10] and AS/NSZ 4673:2001 [11] lead to more unsafe results for welded duplex and ferritic stainless steel columns undergoing minor axis flexural buckling. In the following sections, a series of modifications on the column design method provided in EN 1993-1-4 [9] are made with the aim of achieving more accurate flexural buckling strength predictions for welded duplex and ferritic stainless steel I-section columns. Moreover, the reliability of the new proposals is also verified.

## 5. Proposals for the improvement of the accuracy of the column design method provided in EN 1993-1-4 [9] for welded duplex and ferritic stainless steel I-section columns

### 5.1. Introduction

For the purpose of achieving a higher level of accuracy for the ultimate resistance predictions of welded duplex and ferritic stainless steel I-section columns relative to the existing methods provided in structural stainless design standards and guides [9–12], a series of modifications to the existing column design method provided in EN 1993-1-4 [9] is proposed in this section. In the proposals, the focus is placed upon a proper recalibration of the Perry-Robertson equation given in EN 1993-1-4 [9] for the accurate and safe resistance predictions of welded duplex and ferritic stainless steel I-section columns undergoing flexural buckling.

### 5.2. Recalibration of the Perry-Robertson equation given in EN 1993-1-4 [9] for welded duplex and ferritic stainless steel I-section columns

The flexural buckling reduction factor equation of EN 1993-1-4 [9] given by eq. (10) is recalibrated herein by comparing the generalised imperfection factor  $\eta$  against those determined through the GMNIA of the finite element models  $\eta_{FE}$ , in accordance with the procedure adopted in [31]. The  $\eta_{FE}$  values were determined by rearranging eq. (10) in terms of  $\eta$ , which resulted in the following equation:

$$\eta = \frac{1 - \chi_{FE}}{\chi_{FE}} \left( 1 - \chi_{FE} \bar{\lambda}^2 \right) \quad (21)$$

where  $\chi_{FE}$  is the ratio of the ultimate resistance predictions obtained through the GMNIA of a stainless steel column  $N_{ult,FE}$  to its axial cross-section resistance equal to its cross-section area multiplied by the 0.2% proof strength  $N_{pl} = Af_y$  (i.e.  $\chi_{FE} = N_{ult,FE}/N_{pl}$ ).

Eq. (10) is recalibrated for the major and minor axis flexural buckling assessment of welded duplex and ferritic stainless steel columns, considering all the parameters provided in Table 3. The accuracy of the proposed imperfection factor expressions  $\eta$  against those obtained from GMNIA  $\eta_{FE}$  are illustrated in Fig. 13 for duplex and ferritic stainless steel I-section columns undergoing major axis and minor axis flexural buckling. As can be seen from the figure, the proposed imperfection factor expressions lead to a high level of accuracy.

The modified EN 1993-1-4 [9] design equations proposed in this section are the same as eq. (9) and eq. (10) where the generalised imperfection factor  $\eta$  is determined as given below

$$\eta = \alpha (\bar{\lambda} - \bar{\lambda}_0) . \quad (22)$$

The proposed values of the imperfection factor  $\alpha$  and threshold slenderness  $\bar{\lambda}_0$  are shown in Table 7 for duplex and ferritic stainless steel columns and major and minor axis flexural buckling. In the following subsection, the accuracy of the recalibrated EN 1993-1-4 [9] column buckling equation with respect to the flexural buckling resistance predictions of welded duplex and ferritic I-section columns is investigated.

It should be emphasised that for the design of a column with a particular grade of duplex or ferritic stainless steel, the recalibrated EN 1993-1-4 [9] column buckling design equations with the corresponding imperfection factor  $\alpha$  and threshold slenderness  $\bar{\lambda}_0$  can be used in conjunction with the 0.2% proof strength  $f_y$  and the Young's modulus  $E$  of the particular stainless steel grade. The use of the material properties given in Table 1 is not necessarily recommended for the design of all duplex and ferritic stainless steel columns. Since the standardised material properties put forward in [35] for duplex and ferritic stainless steel were adopted in this paper, which accurately represent the material stress-strain curves of different stainless steel grades falling into the duplex and ferritic stainless steel categories as shown in [35], it is anticipated that the derived flexural buckling curves lead to accurate ultimate strength predictions for columns made of different grades of duplex and ferritic stainless steel.

### 5.3. Accuracy of the proposed column design equations for welded duplex and ferritic stainless steel I-section columns

In Fig. 14, the accuracy of the recalibrated EN 1993-1-4 [9] is assessed for duplex and ferritic stainless steel I-section columns for different non-dimensional slenderness values, major and minor axis buckling, different cross-section aspect ratios and cross-section classes covering all the parameters provided in Table 3. Fig. 14 shows that the modifications proposed for the column design rules of EN 1993-1-4 [9] lead to very accurate ultimate strength predictions for duplex and ferritic stainless steel I-section columns for all the considered cases. The level of accuracy of the recalibrated EN 1993-1-4 [9] column design equations is also shown in Fig. 15, where its very high accuracy and safety can also be observed.

The accuracy of the recalibrated EN 1993-1-4 [9] design equation is also statistically assessed in Table 8, using the ultimate strengths of duplex and ferritic I-section stainless steel columns obtained from the GMNIA including the parameters provided in Table 3 and those from the experiments of [13, 15, 19]. Table 8 shows that the proposals made in this



paper lead to more accurate flexural buckling resistance predictions for duplex and ferritic stainless steel I-section columns relative to the existing column design methods provided in current stainless steel structural design standards and guides [9–12]. In the following subsection, the reliability of the new proposals is investigated.

## 6. Reliability analysis

In this section, the reliability of the recalibrated EN 1993-1-4 [9] column design equation is assessed through the procedure given in Annex D of EN 1990 [46] for duplex and ferritic stainless steel I-section columns, utilising the numerical results generated in this study and the experimental results collected from [13, 15, 19]. The important parameters of the reliability analysis are illustrated in Table 9 considering the benchmark ultimate resistance predictions from only numerical models, experiments [13, 15, 19] and from both numerical models and experiments. In Table 9,  $N$  is the number of the considered numerical and experimental data,  $b$  is the mean value correction factor,  $k_{d,n}$  is the fractile factor which is dependent upon the number of the data considered and  $V_\delta$  is the coefficient of variation of the experimental and numerical ultimate strengths relative to the resistance prediction. Note that the mean correction factor  $b$  was determined herein by taking the average of the ratios of the experimental and numerical ultimate resistances to those predicted by the proposed design method; unlike the least squares approach recommended in EN 1990 [46], this avoids the bias of  $b$  towards the experimental or numerical results with larger ultimate resistances [29, 47]. In accordance with the recommendations provided in [47], the material overstrength factors, defined as the ratio of the mean yield strength  $f_{y,mean}$  to the nominal yield strength  $f_{y,nom}$ , were taken as  $f_{y,mean}/f_{y,nom} = 1.10$  and  $f_{y,mean}/f_{y,nom} = 1.20$  for duplex and ferritic stainless steel, respectively. Moreover, the coefficient of variation of the geometry  $V_{geometry}$  was taken as 0.05 (i.e.  $V_{geometry} = 0.05$ ) and the coefficients of variation of the yield strength  $V_{fy}$  were taken as 0.03 and 0.045 for duplex and ferritic stainless steel as recommended in [47] (i.e.  $V_{fy} = 0.03$  for duplex stainless steel and  $V_{fy} = 0.045$  for ferritic stainless steel).

Table 9 shows that the determined partial safety factors  $\gamma_{M1}$  for the recalibrated EN 1993-1-4 [9] column buckling design equation are generally very close to or lower than the partial safety factor value of  $\gamma_{M1} = 1.10$  recommended in EN 1993-1-4 [9], highlighting that the recalibrated EN 1993-1-4 [9] column buckling design equation can be safely adopted for the design of duplex and ferritic stainless steel beam-columns susceptible to flexural buckling. It should be emphasised that the partial safety factors  $\gamma_{M1}$  determined according to the procedure given in Annex D of EN 1990 [46] can be very sensitive to the variations and number of the benchmark data which were obtained through GMNIA and physical experiments from the literature [13, 15, 19] in this paper. When only the test results are considered for duplex stainless steel columns undergoing major axis buckling, the partial safety factor  $\gamma_{M1}$  determined for the recalibrated EN 1993-1-4 [9] column design method is higher than  $\gamma_{M1} = 1.10$ ; this is due to the low number and variation of the test data obtained from two different experimental studies [13, 15]. When the data from both GMNIA and experiments are considered, the partial safety factor for the recalibrated EN 1993-1-4 [9] column design method for the major axis buckling assessment of duplex stainless steel

I-section columns becomes  $\gamma_{M1} = 1.07$ , which is smaller than the partial safety factor value  $\gamma_{M1} = 1.10$  adopted in EN 1993-1-4 [9]. However, it should also be noted that in the GMNIA of the finite element models, a series of idealised features for the columns such as perfectly applied concentric axial compression, perfect pin-ended boundary conditions and consistent global and local geometric imperfection patterns and magnitudes described in Section 2.2 were assumed. In the experimental studies and in actual stainless steel structures, these idealised features invariably do not exist for duplex and ferritic stainless steel columns. In the reliability analyses, this results in higher coefficient of variation  $V_\delta$  values when the results from the experiments are considered relative to those obtained considering the results from the finite element analyses, which can be seen in Table 9. Thus, it suffices to state that the partial safety factors  $\gamma_{M1}$  determined considering the experimental results in this subsection provide a more realistic representation of the reliability level of the recalibrated EN 1993-1-4 [9] column buckling design equation which are smaller than the recommended value of  $\gamma_{M1} = 1.10$  in EN 1993-1-4 [9] for all the cases with the exception of the major axis flexural buckling assessment of duplex stainless steel I-section columns; as indicated, this results from the low number and variation of the test results observed in two different experimental studies [13, 15].

The partial safety factors determined for the column buckling design equation of EN 1993-1-4 [9] are provided in Table 10, showing that the partial safety factors  $\gamma_{M1}$  determined for the existing column design equations of EN 1993-1-4 [9] are also very close to or less than  $\gamma_{M1} = 1.10$  for duplex and ferritic stainless steel columns undergoing major and minor axis buckling. As can be seen from Table 10, even though EN 1993-1-4 [9] leads to quite conservative ultimate strength predictions for duplex stainless steel columns, the partial safety factor determined considering only the test data for the major axis buckling assessment of duplex stainless steel columns is also significantly higher than  $\gamma_{M1} = 1.10$  adopted in EN 1993-1-4 [9]; this is again due to the low number and variation of the test data obtained from two different studies [13, 15] for this case. The same observation can also be made for the partial safety factors determined for the recalibrated and original EN 1993-1-4 [9] column buckling equations for the minor axis flexural buckling assessment of ferritic stainless steel columns when the data from both the finite element models and experiments of [19] are considered. However, for both the recalibrated EN 1993-1-4 [9] column design equation and the original EN 1993-1-4 [9] column design equation, the partial safety factors are very close to or lower than the partial safety factor value of  $\gamma_{M1} = 1.10$  recommended in EN 1993-1-4 [9] when a high number of consistent data from the GMNIA and experiments are taken into consideration, indicating that both methods can be applied for the flexural buckling assessment of duplex and stainless steel I-section columns by adopting a partial safety factor  $\gamma_{M1}$  value of 1.10 (i.e.  $\gamma_{M1} = 1.10$ ).

## 7. Conclusions

The flexural buckling behaviour and design of welded duplex and ferritic stainless I-section columns were investigated in this paper. Finite element models able to replicate the structural response of duplex and ferritic stainless steel columns were created and vali-

dated against experimental results from the literature. Through the validated finite element models, extensive numerical parametric studies were carried out to generate comprehensive structural performance data for duplex and ferritic stainless steel columns undergoing flexural buckling. Importance of a series of parameters on the behaviour of welded stainless steel I-section columns was illustrated. Using experimental data collected from the literature and numerical data obtained from extensive numerical parametric studies, the accuracy and reliability of the existing column design methods provided in structural stainless steel design standards and guides such as EN 1993-1-4 [9], AISC Design Guide 27 [12], ASCE/SEI-8 [10] and AS/NSZ 4673:2001 [11] for the flexural buckling assessment of duplex and ferritic stainless steel I-section columns were investigated. It was observed that while EN 1993-1-4 [9] leads to the most accurate and reliable results relative to the existing stainless steel design standards and guides, it still provides overly conservative ultimate strength predictions in some cases. The results also indicated that AISC Design Guide 27 [12] leads to very uneconomic and overly-conservative results for duplex and ferritic stainless steel I-section columns, while ASCE/SEI-8 [10] and AS/NSZ 4673:2001 [11] provide unsafe ultimate strength predictions for such members. The unsafe ultimate strength predictions of ASCE/SEI-8 [10] and AS/NSZ 4673:2001 [11] were ascribed to the fact that the column design methods given in these standards were originally developed for cold-formed stainless steel structural elements and the presence of residual stresses within duplex and ferritic stainless steel I-section columns can lead to considerable reductions in their ultimate strengths, which are not taken into account by ASCE/SEI-8 [10] and AS/NSZ 4673:2001 [11]. For the purpose of improving the accuracy of the column design method provided in EN 1993-1-4 [9] for duplex and ferritic stainless steel I-section columns, its recalibration was carried out in this paper. It was shown that the recalibrated EN 1993-1-4 [9] column design equation leads to more accurate flexural buckling strength predictions for duplex and ferritic stainless steel I-section columns relative to the column design methods in existing stainless steel design standards and guides [9–12]. The reliability of the recalibrated EN 1993-1-4 [9] column design equations was also provided in line with the procedure recommended in Annex D of EN 1990 [46]. Future research will be directed towards the behaviour and design of duplex and ferritic stainless steel I-section beam-columns.

## References

- [1] Gardner, L., Nethercot, D.A.. Experiments on stainless steel hollow sections—Part 1: Material and cross-sectional behaviour. *Journal of Constructional Steel Research* 2004;60(9):1291–1318.
- [2] Gardner, L., Nethercot, D.A.. Experiments on stainless steel hollow sections—Part 2: Member behaviour of columns and beams. *Journal of Constructional Steel Research* 2004;60(9):1319–1332.
- [3] Young, B., Lui, W.M.. Behavior of cold-formed high strength stainless steel sections. *Journal of Structural Engineering, ASCE* 2005;131(11):1738–1745.
- [4] Becque, J., Rasmussen, K.J.. Experimental investigation of local-overall interaction buckling of stainless steel lipped channel columns. *Journal of Constructional Steel Research* 2009;65(8-9):1677–1684.
- [5] Rossi, B., Jaspart, J.P., Rasmussen, K.J.. Combined distortional and overall flexural-torsional buckling of cold-formed stainless steel sections: Experimental investigations. *Journal of Structural Engineering, ASCE* 2009;136(4):354–360.

- [6] Huang, Y., Young, B.. Experimental and numerical investigation of cold-formed lean duplex stainless steel flexural members. *Thin-Walled Structures* 2013;73:216–228.
- [7] Huang, Y., Young, B.. Experimental investigation of cold-formed lean duplex stainless steel beam-columns. *Thin-Walled Structures* 2014;76:105–117.
- [8] Gardner, L.. Stability and design of stainless steel structures—Review and outlook. *Thin-Walled Structures* 2019;141:208–216.
- [9] EN 1993-1-4, Eurocode 3 Design of steel structures-Part 1-4: General rules – Supplementary rules for stainless steel. European Committee for Standardization (CEN), Brussels; 2015.
- [10] SEI/ASCE 8-02, Specification for the design of cold-formed stainless steel structural members. American Society of Civil Engineers (ASCE), Reston; 2002.
- [11] AS/NZS 4673, Cold-formed stainless steel structures. Australian/New Zealand Standard, Sydney; 2001.
- [12] AISC Design Guide 27: Structural Stainless Steel. American Institute of Steel Construction (AISC), Chicago, Illinois, USA; 2013.
- [13] Yang, L., Zhao, M., Chan, T.M., Shang, F., Xu, D.. Flexural buckling of welded austenitic and duplex stainless steel I-section columns. *Journal of Constructional Steel Research* 2016;122:339–353.
- [14] Yang, L., Zhao, M., Gardner, L., Ning, K., Wang, J.. Member stability of stainless steel welded I-section beam-columns. *Journal of Constructional Steel Research* 2019;155:33–45.
- [15] Burgan, B., Baddoo, N., Gilsenan, K.. Structural design of stainless steel members—Comparison between Eurocode 3, Part 1.4 and test results. *Journal of Constructional Steel Research* 2000;54(1):51–73.
- [16] Zheng, B., Hua, X., Shu, G.. Tests of cold-formed and welded stainless steel beam-columns. *Journal of Constructional Steel Research* 2015;111:1–10.
- [17] Ahmed, S., Al-Deen, S., Ashraf, M.. Design rules for stainless steel welded I-columns based on experimental and numerical studies. *Engineering Structures* 2018;172:850–868.
- [18] Yuan, H., Wang, Y., Shi, Y., Gardner, L.. Residual stress distributions in welded stainless steel sections. *Thin-Walled Structures* 2014;79:38–51.
- [19] Bredenkamp, P., Van den Berg, G.. The strength of stainless steel built-up I-section columns. *Journal of Constructional Steel Research* 1995;34(2-3):131–144.
- [20] Yang, L., Wang, Y., Gao, B., Shi, Y., Yuan, H.. Two calculation methods for buckling reduction factors of stainless steel welded I-section beams. *Thin-Walled Structures* 2014;83:128–136.
- [21] Wang, Y., Yang, L., Gao, B., Shi, Y., Yuan, H.. Experimental study of lateral-torsional buckling behavior of stainless steel welded I-section beams. *International Journal of Steel Structures* 2014;14(2):411–420.
- [22] Gardner, L., Bu, Y., Theofanous, M.. Laser-welded stainless steel I-sections: Residual stress measurements and column buckling tests. *Engineering Structures* 2016;127:536–548.
- [23] Bu, Y., Gardner, L.. Local stability of laser-welded stainless steel I-sections in bending. *Journal of Constructional Steel Research* 2018;148:49–64.
- [24] Bu, Y., Gardner, L.. Laser-welded stainless steel I-section beam-columns: Testing, simulation and design. *Engineering Structures* 2019;179:23–36.
- [25] Bu, Y., Gardner, L.. Finite element modelling and design of welded stainless steel I-section columns. *Journal of Constructional Steel Research* 2019;152:57–67.
- [26] Saliba, N., Gardner, L.. Cross-section stability of lean duplex stainless steel welded I-sections. *Journal of Constructional Steel Research* 2013;80:1–14.
- [27] Yuan, H., Wang, Y., Shi, Y., Gardner, L.. Stub column tests on stainless steel built-up sections. *Thin-Walled Structures* 2014;83:103–114.
- [28] Yuan, H., Wang, Y., Gardner, L., Du, X., Shi, Y.. Local–overall interactive buckling behaviour of welded stainless steel I-section columns. *Journal of Constructional Steel Research* 2015;111:75–87.
- [29] Kucukler, M., Gardner, L., Bu, Y.. Flexural-torsional buckling of austenitic stainless steel i-section beam-columns: Testing, numerical modelling and design. *Thin-Walled Structures* 2020;152:106572.
- [30] Abaqus 2018 Reference Manual. Simulia, Dassault Systemes; 2018.
- [31] Kucukler, M., Gardner, L., Macorini, L.. Lateral–torsional buckling assessment of steel beams

- through a stiffness reduction method. *Journal of Constructional Steel Research* 2015;109:87–100.
- [32] Kucukler, M., Gardner, L., Macorini, L.. Flexural–torsional buckling assessment of steel beam–columns through a stiffness reduction method. *Engineering Structures* 2015;101:662–676.
  - [33] Kucukler, M., Gardner, L.. Design of web-tapered steel beams against lateral-torsional buckling through a stiffness reduction method. *Engineering Structures* 2019;190:246–261.
  - [34] Kucukler, M., Xing, Z., Gardner, L.. Behaviour and design of stainless steel I-section columns in fire. *Journal of Constructional Steel Research* 2020;165:105890.
  - [35] Afshan, S., Zhao, O., Gardner, L.. Standardised material properties for numerical parametric studies of stainless steel structures and buckling curves for tubular columns. *Journal of Constructional Steel Research* 2019;152:2–11.
  - [36] Dawson, R.G., Walker, A.C.. Post-buckling of geometrically imperfect plates. *Journal of the Structural Division, ASCE* 1972;98(1):75–94.
  - [37] Gardner, L., Nethercot, D.. Numerical modeling of stainless steel structural components—a consistent approach. *Journal of Structural Engineering, ASCE* 2004;130(10):1586–1601.
  - [38] Ashraf, M., Gardner, L., Nethercot, D.A.. Finite element modelling of structural stainless steel cross-sections. *Thin-walled structures* 2006;44(10):1048–1062.
  - [39] Jandera, M., Gardner, L., Machacek, J.. Residual stresses in cold-rolled stainless steel hollow sections. *Journal of Constructional Steel Research* 2008;64(11):1255–1263.
  - [40] EN 1993-1-1, Eurocode 3 Design of steel structures-Part 1-1: General rules and rules for buildings. European Committee for Standardization (CEN), Brussels; 2005.
  - [41] Ayrton, W., Perry, J.. On struts. *The Engineer* 1886;62:464–465.
  - [42] Robertson, A.. The strength of struts. *The Institution of Civil Engineers (ICE) – Selected Engineering Papers* 1925;1(28):1–55.
  - [43] Surovek-Maleck, A.E., White, D.W.. Alternative approaches for elastic analysis and design of steel frames. I: Overview. *Journal of Structural Engineering, ASCE* 2004;130(8):1186–1196.
  - [44] Kucukler, M., Gardner, L., Macorini, L.. Development and assessment of a practical stiffness reduction method for the in-plane design of steel frames. *Journal of Constructional Steel Research* 2016;126:187–200.
  - [45] Kucukler, M., Gardner, L.. Design of laterally restrained web-tapered steel structures through a stiffness reduction method. *Journal of Constructional Steel Research* 2018;141:63–76.
  - [46] EN 1990, Basis for structural design. European Committee for Standardization (CEN), Brussels; 2005.
  - [47] Afshan, S., Francis, P., Baddoo, N., Gardner, L.. Reliability analysis of structural stainless steel design provisions. *Journal of Constructional Steel Research* 2015;114:293–304.

## Figures captions

Figure 1 : Two-stage compound Ramberg-Osgood material model and stress-strain response for duplex and ferritic stainless steel adopted in this study

Figure 2 : Lowest local and global buckling modes used to apply geometric imperfections to finite element models

Figure 3 : Residual stress pattern adopted for welded stainless steel I-sections (+ve = tension, -ve = compression)

Figure 4 : Comparison of axial compression versus deformation paths obtained from experiments of Yang et al. [13] and finite element models for specimens subjected to major axis flexural buckling

Figure 5 : Comparison of axial compression versus deformation paths obtained from experiments of Yang et al. [13] and finite element models for specimens subjected to minor axis flexural buckling

Figure 6 : Comparison of the failure mode of the specimen I2205-2000 observed in the experiment of Yang et al. [13] against the failure mode obtained from its finite element model created in this study

Figure 7 : Comparison of the ultimate strengths of ferritic stainless steel I-section columns observed in the experiments of [19] and those determined through the finite element models of the specimens created in this study

Figure 8 : Influence of a stainless steel grade on the normalised resistances of stainless steel I-section columns

Figure 9 : Influence of the axis of buckling on the normalised resistances of duplex and ferritic stainless steel I-section columns

Figure 10 : Influence of the cross-section aspect ratio on the normalised resistances of duplex and ferritic stainless steel I-section columns

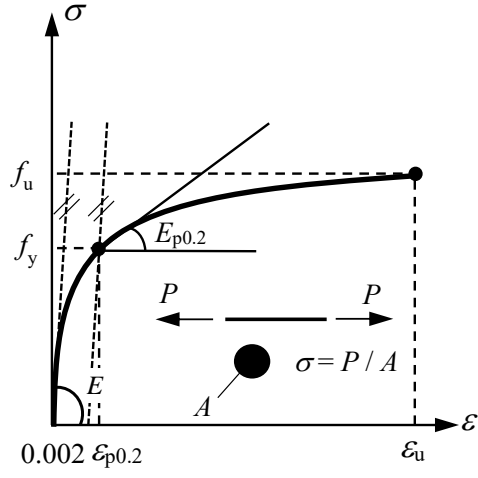
Figure 11 : Comparison of ultimate strength predictions obtained from GMNIA against those determined through EN 1993-1-4 [9] and AISC Design Guide 27 [12] for duplex and ferritic stainless steel I-section columns undergoing major and minor axis buckling

Figure 12 : Accuracy of EN 1993-1-4 [9], AISC Design Guide 27 [12], ASCE/SEI-8 [10] and AS/NZS 4673:2001 [11] for ultimate strength predictions of duplex and ferritic stainless steel I-section columns undergoing major and minor axis buckling

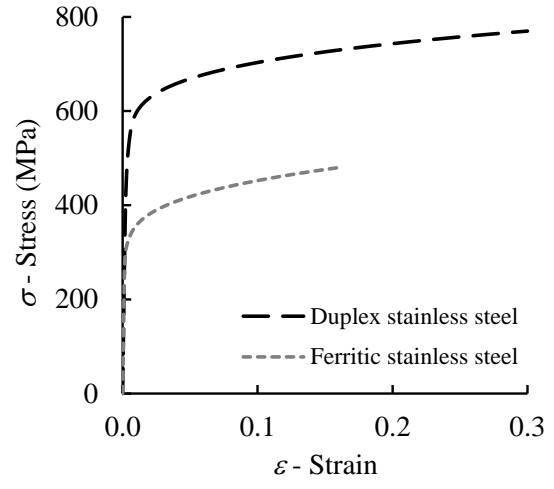
Figure 13 : Recalibration of the Perry-Robertson equation provided in EN 1993-1-4 [9] for welded duplex and ferritic stainless steel I-section columns

Figure 14 : Accuracy of the the recalibrated EN 1993-1-4 [9] column design equation for welded duplex and ferritic stainless steel I-section columns

Figure 15 : Accuracy of the proposed column design equations for ultimate strength predictions of duplex and ferritic stainless steel columns undergoing major and minor axis buckling



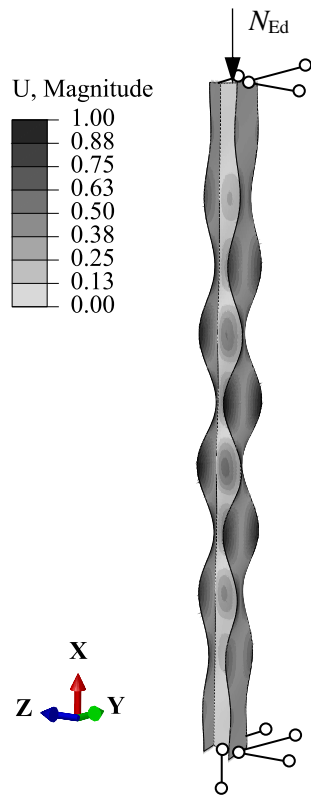
(a) Material model



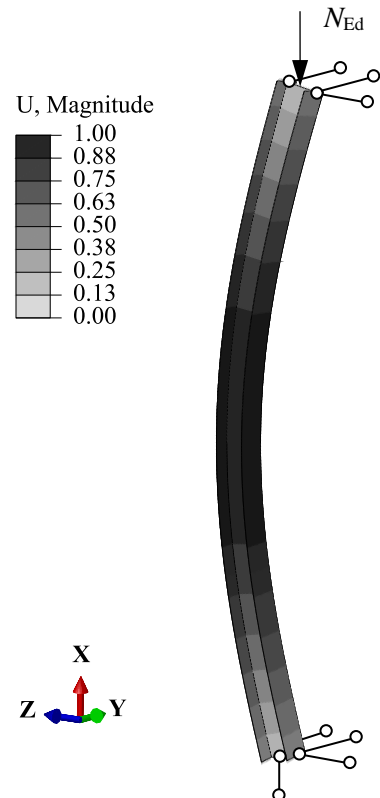
(b) Stress-strain curves

Figure 1: Two-stage compound Ramberg-Osgood material model and stress-strain response for duplex and ferritic stainless steel adopted in this study





(a) Lowest local buckling mode



(b) Lowest global buckling mode

Figure 2: Lowest local and global buckling modes used to apply geometric imperfections to finite element models

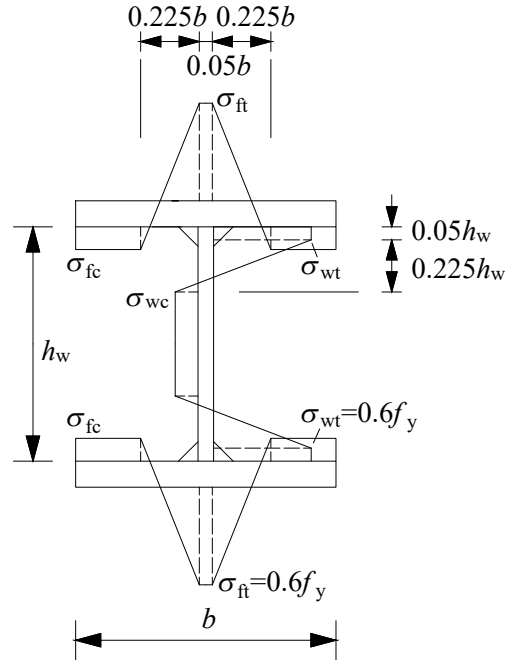


Figure 3: Residual stress pattern adopted for welded stainless steel I-sections (+ve = tension, -ve = compression)

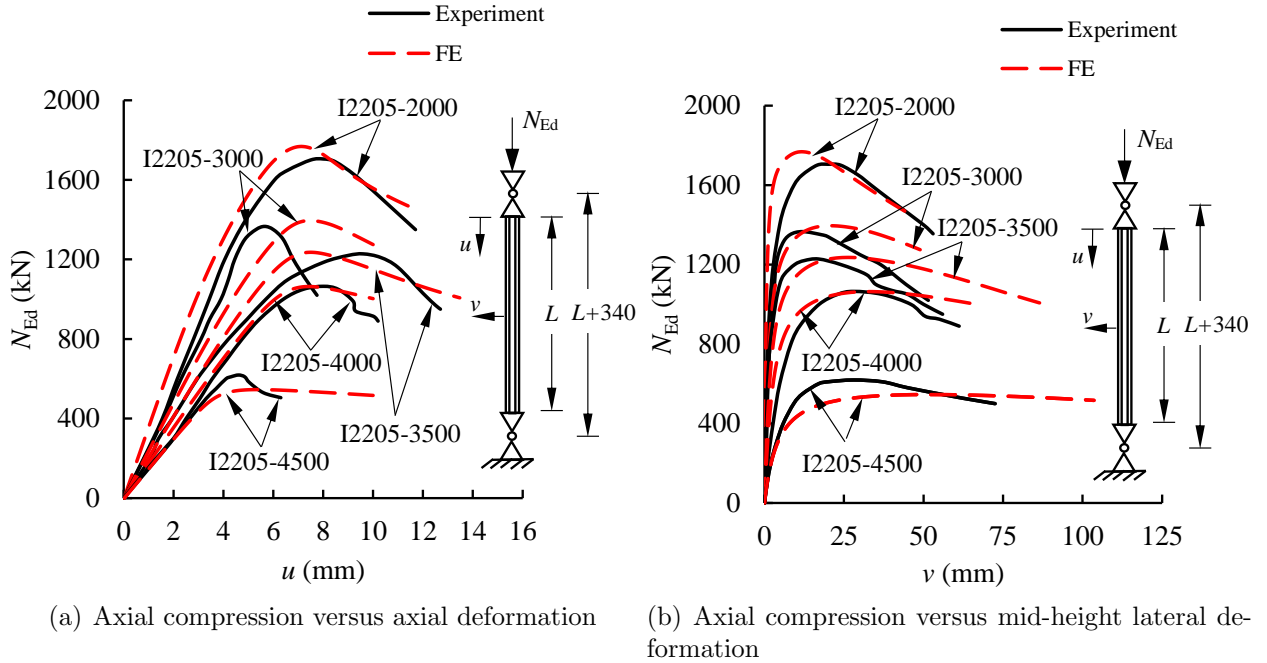


Figure 4: Comparison of axial compression versus deformation paths obtained from experiments of Yang et al. [13] and finite element models for specimens subjected to major axis flexural buckling

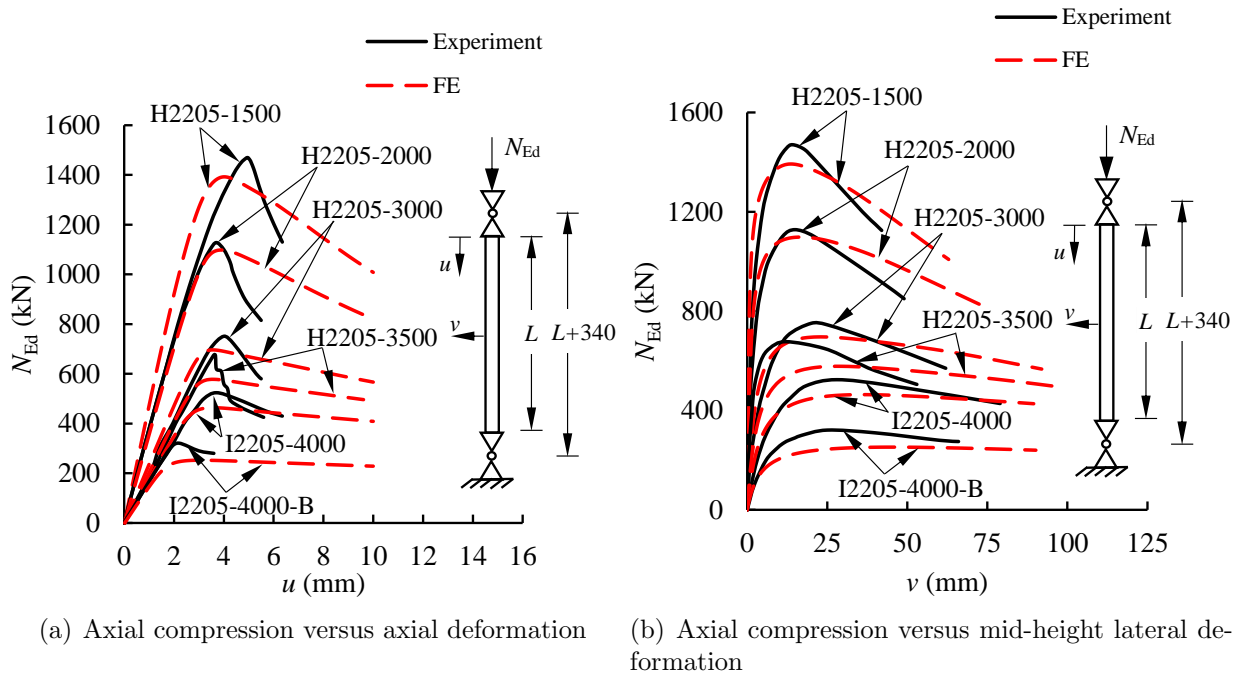


Figure 5: Comparison of axial compression versus deformation paths obtained from experiments of Yang et al. [13] and finite element models for specimens subjected to minor axis flexural buckling



(a) Experimental failure mode



(b) Numerical failure mode

Figure 6: Comparison of the failure mode of the specimen I2205-2000 observed in the experiment of Yang et al. [13] against the failure mode obtained from its finite element model created in this study

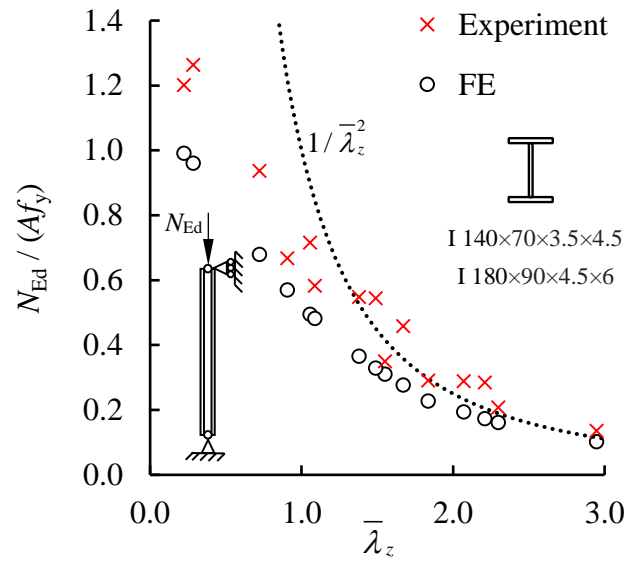


Figure 7: Comparison of the ultimate strengths of ferritic stainless steel I-section columns observed in the experiments of [19] and those determined through the finite element models of the specimens created in this study

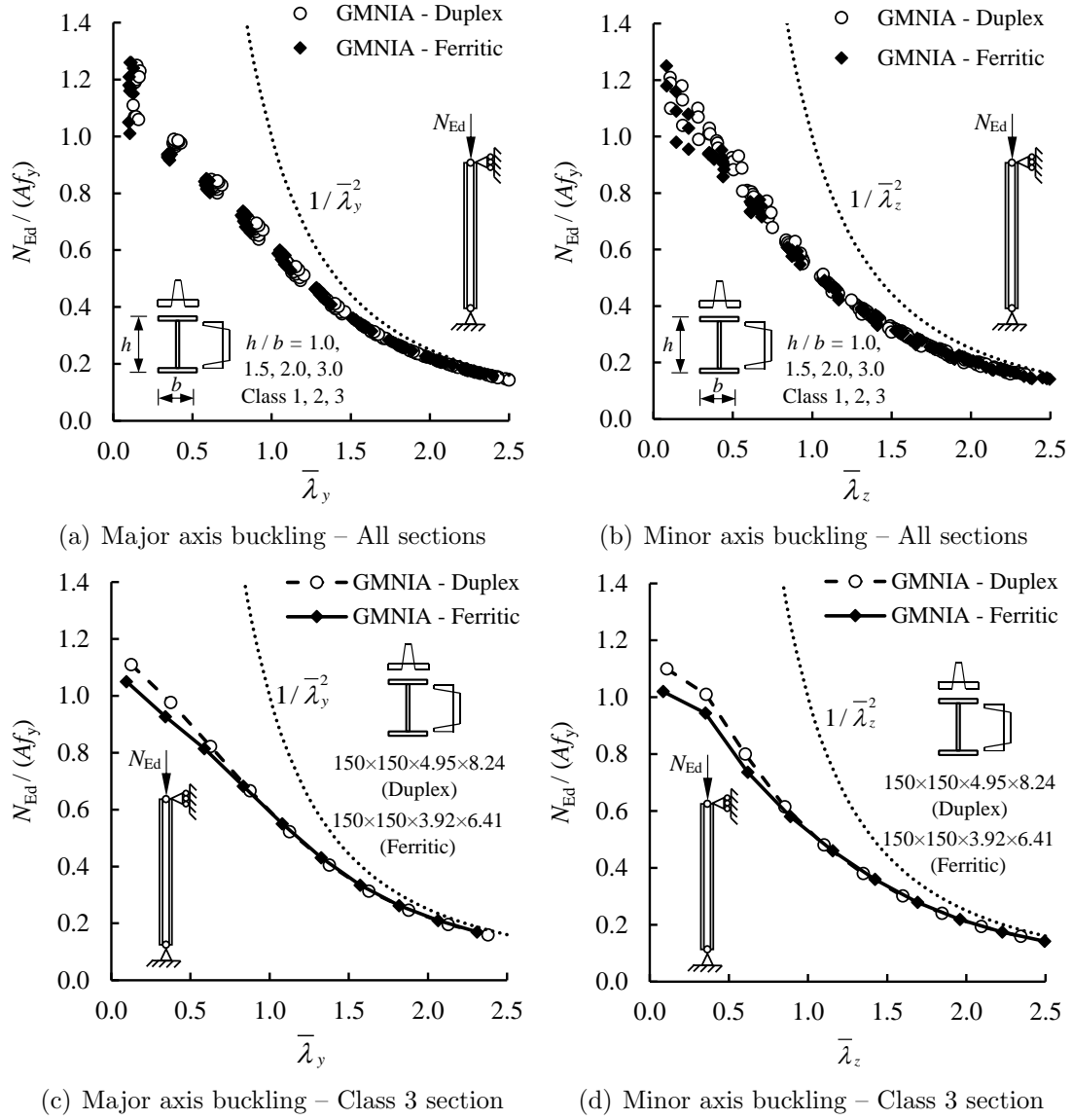


Figure 8: Influence of a stainless steel grade on the normalised resistances of stainless steel I-section columns

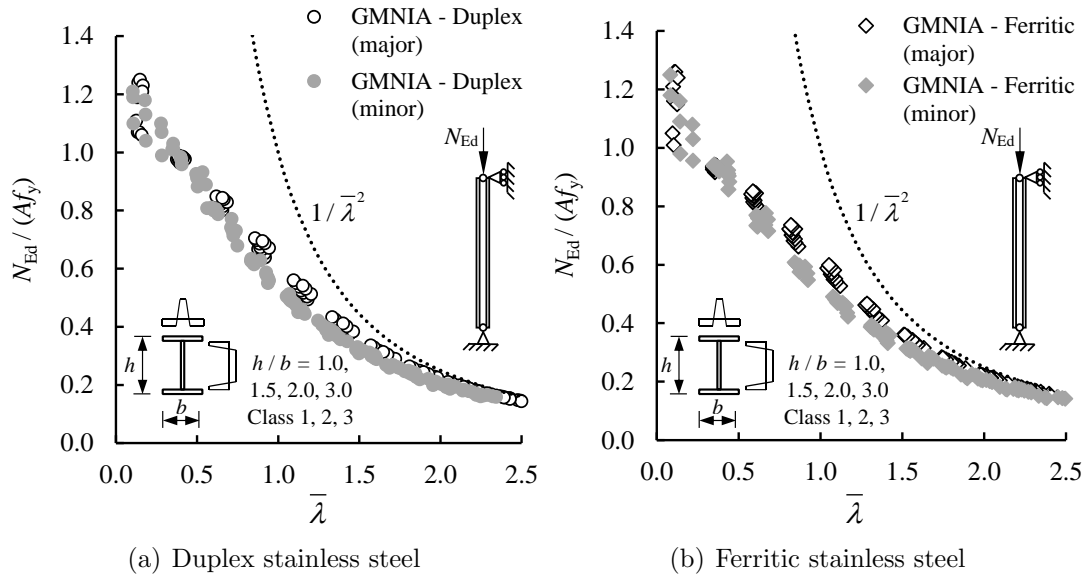
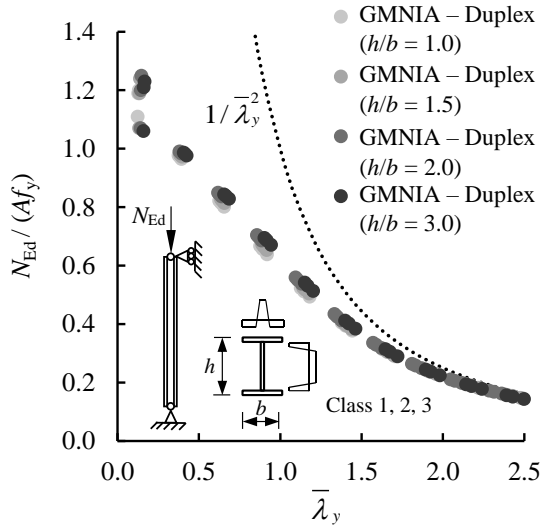
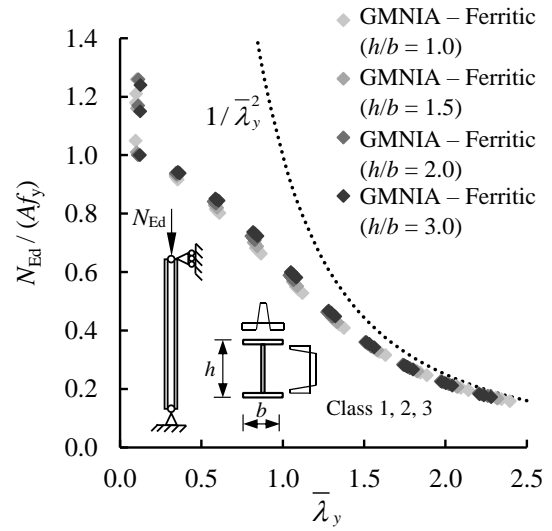


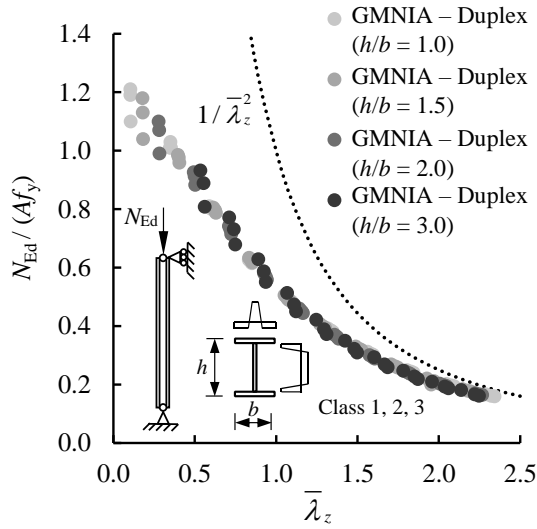
Figure 9: Influence of the axis of buckling on the normalised resistances of duplex and ferritic stainless steel I-section columns



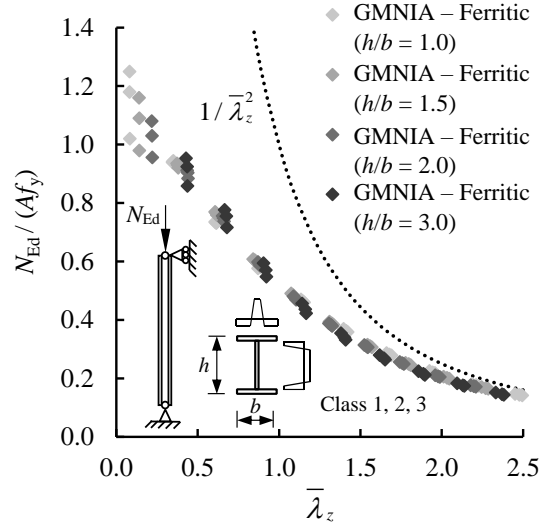
(a) Duplex stainless steel columns – Major axis buckling



(b) Ferritic stainless steel columns – Major axis buckling



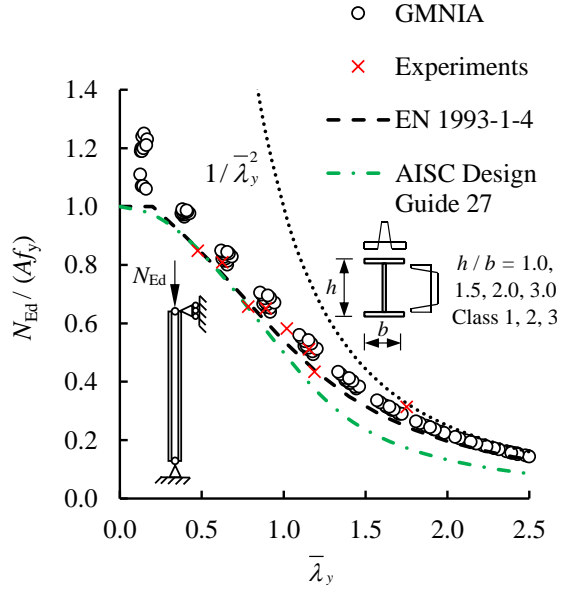
(c) Duplex stainless steel columns – Minor axis buckling



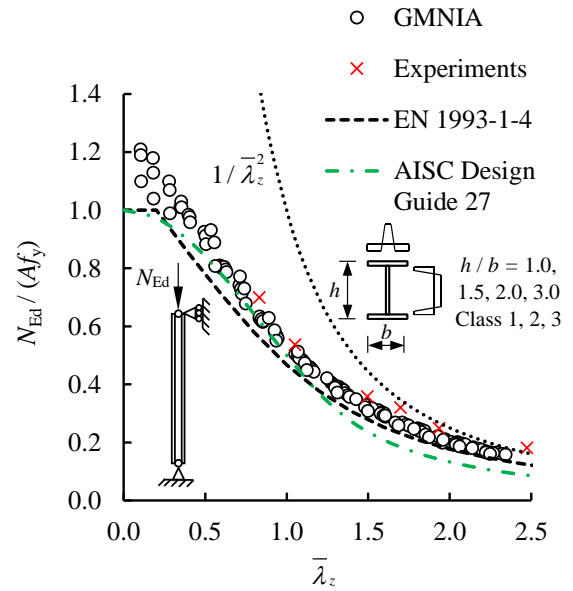
(d) Ferritic stainless steel columns – Minor axis buckling

Figure 10: Influence of the cross-section aspect ratio on the normalised resistances of duplex and ferritic stainless steel I-section columns

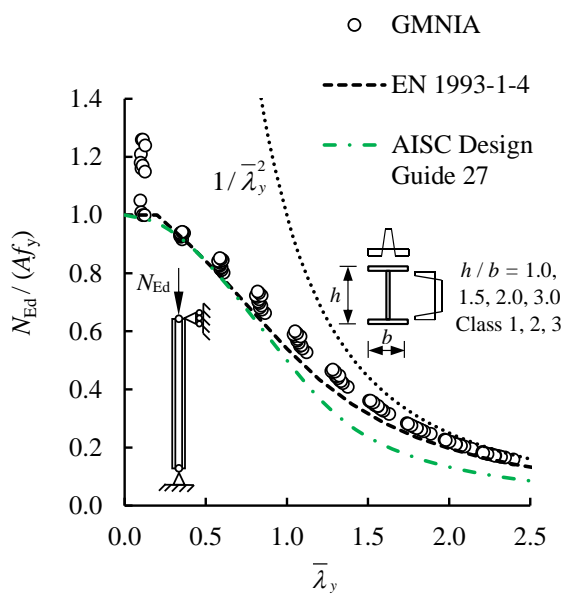




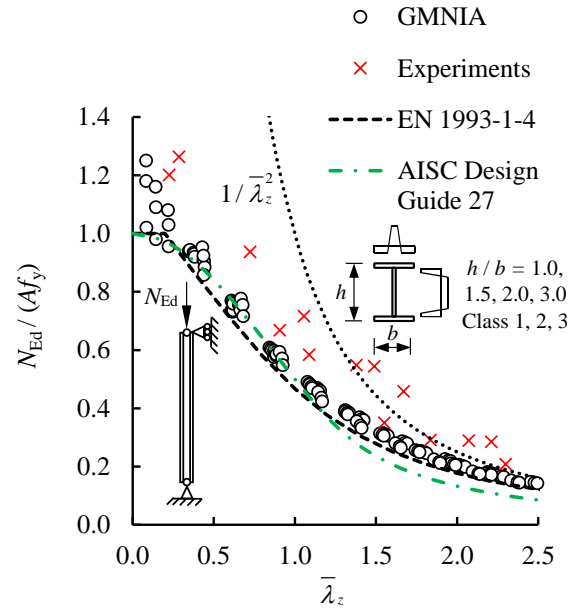
(a) Duplex stainless steel columns – Major axis buckling



(b) Duplex stainless steel columns – Minor axis buckling



(c) Ferritic stainless steel columns – Major axis buckling



(d) Ferritic stainless steel columns – Minor axis buckling

Figure 11: Comparison of ultimate strength predictions obtained from GMNIA against those determined through EN 1993-1-4 [9] and AISC Design Guide 27 [12] for duplex and ferritic stainless steel I-section columns undergoing major and minor axis buckling

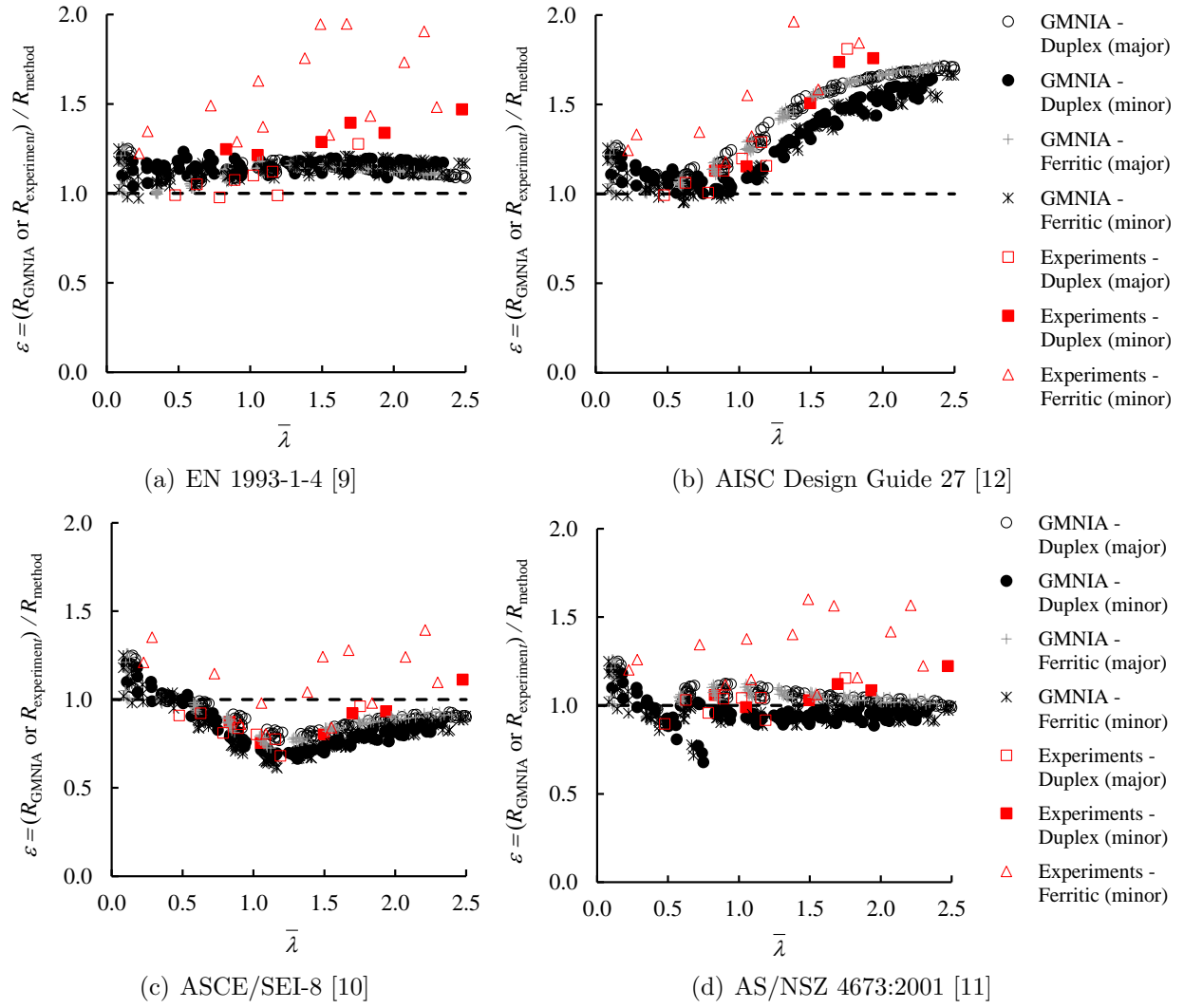
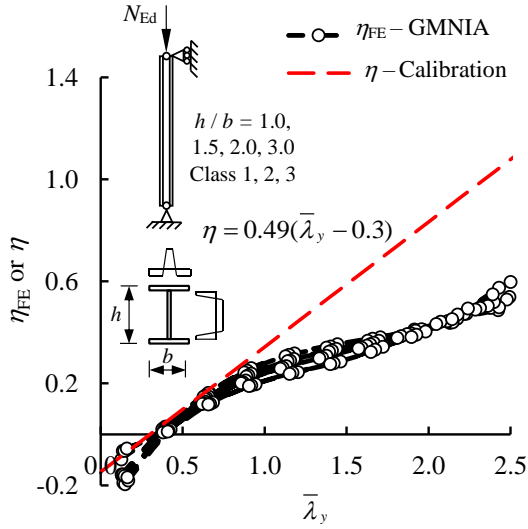
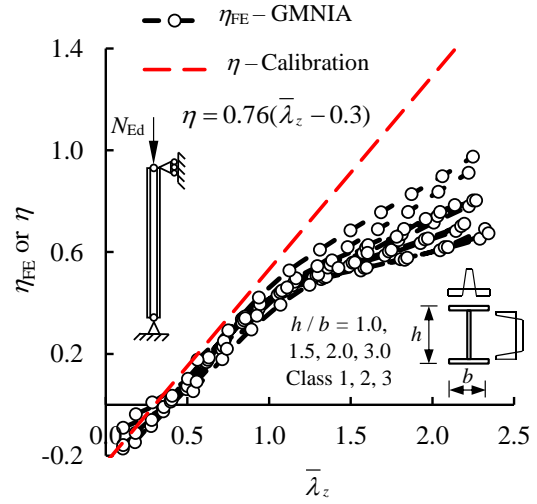


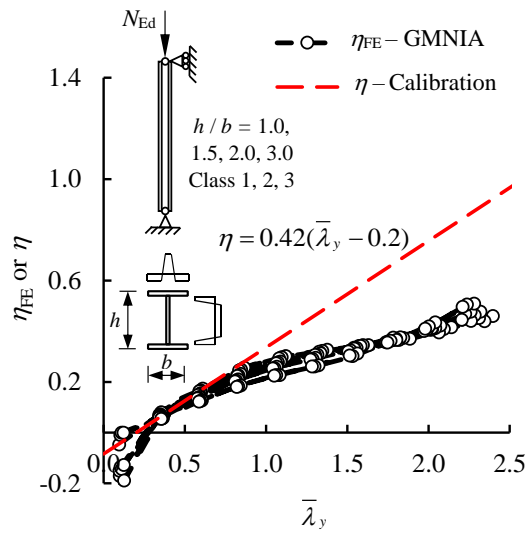
Figure 12: Accuracy of EN 1993-1-4 [9], AISC Design Guide 27 [12], ASCE/SEI-8 [10] and AS/NZS 4673:2001 [11] for ultimate strength predictions of duplex and ferritic stainless steel I-section columns undergoing major and minor axis buckling



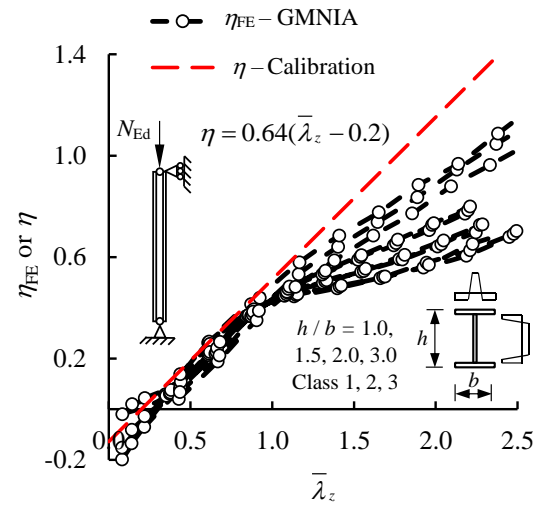
(a) Duplex stainless steel columns – Major axis buckling



(b) Duplex stainless steel columns – Minor axis buckling

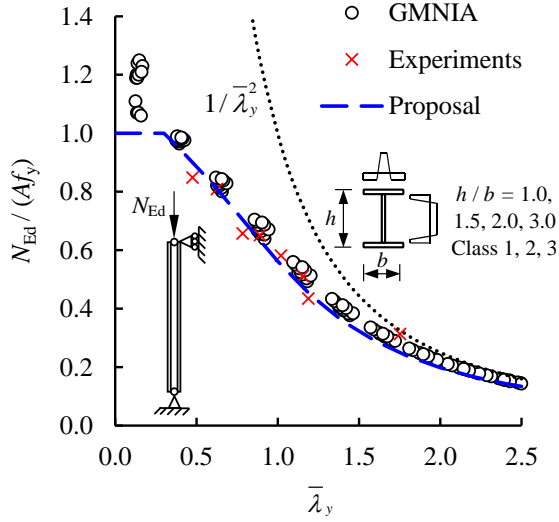


(c) Ferritic stainless steel columns – Major axis buckling

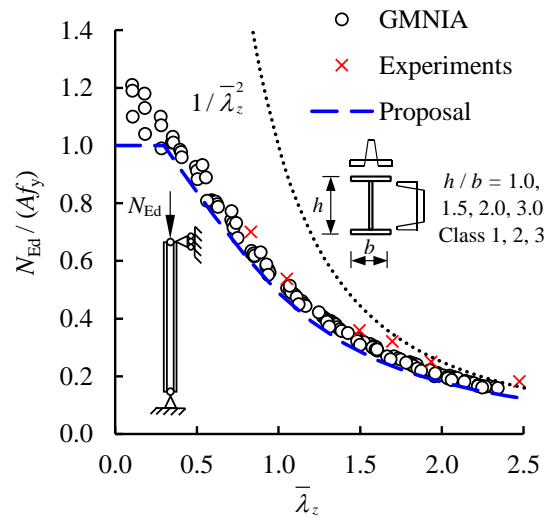


(d) Ferritic stainless steel columns – Minor axis buckling

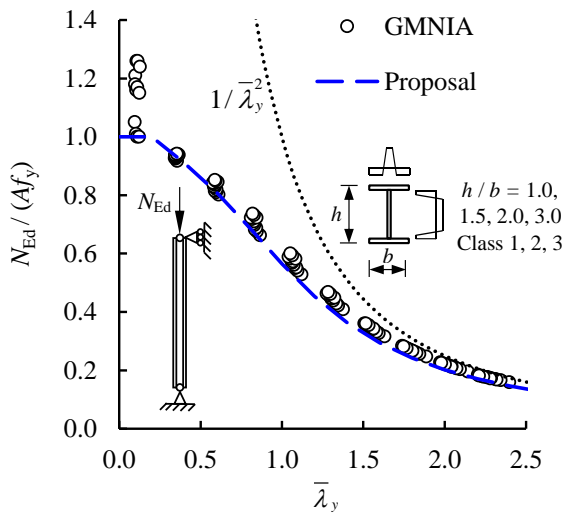
Figure 13: Recalibration of the Perry-Robertson equation provided in EN 1993-1-4 [9] for welded duplex and ferritic stainless steel I-section columns



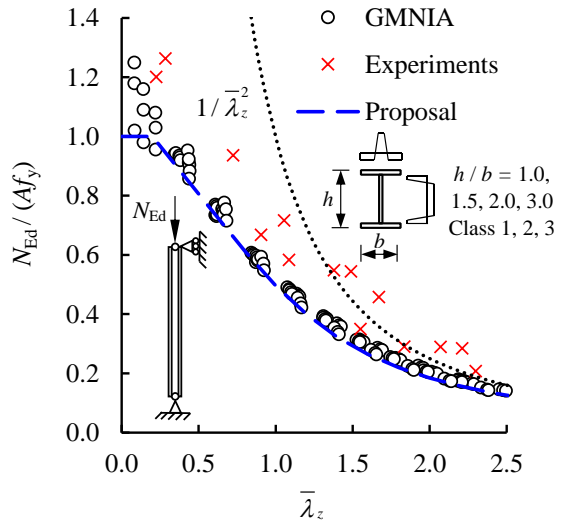
(a) Duplex stainless steel columns – Major axis buckling



(b) Duplex stainless steel columns – Minor axis buckling



(c) Ferritic stainless steel columns – Major axis buckling



(d) Ferritic stainless steel columns – Minor axis buckling

Figure 14: Accuracy of the the recalibrated EN 1993-1-4 [9] column design equation for welded duplex and ferritic stainless steel I-section columns

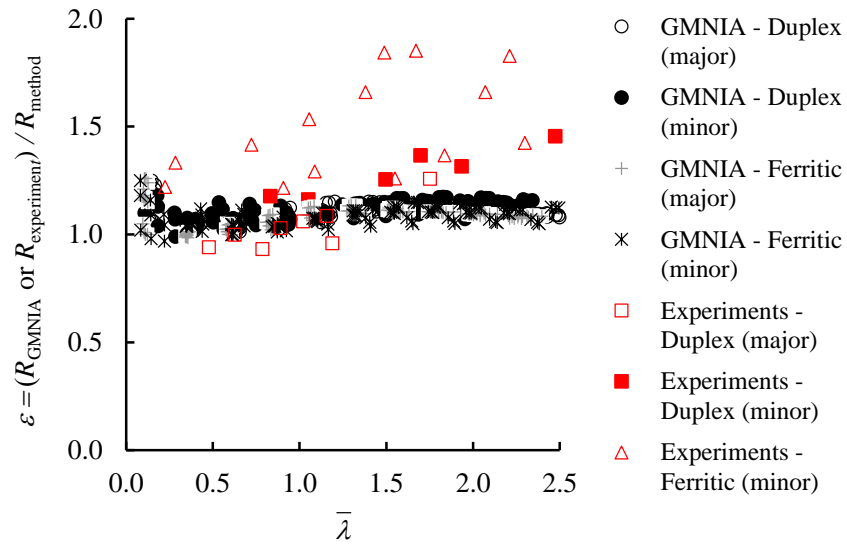


Figure 15: Accuracy of the proposed column design equations for ultimate strength predictions of duplex and ferritic stainless steel columns undergoing major and minor axis buckling

## Tables captions

Table 1 : Material properties used to define the stress-strain response of duplex and ferritic stainless steel in this study

Table 2 : Comparison of the ultimate strengths of duplex stainless steel I-section columns obtained in the experiments of [13, 15] and those determined through the finite element models of the specimens created in this study

Table 3 : Summary of parametric studies carried out in this paper

Table 4 : Imperfection factor  $\alpha$  and threshold slenderness  $\bar{\lambda}_0$  values recommended by EN 1993-1-4 [9] for welded stainless steel I-section columns

Table 5 : The values of the parameters  $\alpha$ ,  $\beta$ ,  $\lambda_0$ ,  $\lambda_1$  and  $E_0$  recommended by Australian & New Zealandian AS/NSZ 4673:2001 [11] for stainless steel columns

Table 6 : Accuracy of EN 1993-1-4 [9], AISC Design Guide 27 [12], ASCE/SEI-8 [10] and AS/NSZ 4673:2001 [11] for ultimate strength predictions of welded duplex and ferritic stainless steel I-section columns

Table 7 : Proposed imperfection factor  $\alpha$  and threshold slenderness  $\bar{\lambda}_0$  values for welded duplex and ferritic stainless steel I-section columns

Table 8 : Accuracy of the recalibrated column design method of EN 1993-1-4 [9] for welded duplex and ferritic stainless steel I-section columns

Table 9 : Reliability analysis of the recalibrated column design method of EN 1993-1-4 [9] for welded duplex and ferritic stainless steel I-section columns

Table 10 : Reliability analysis of the column design method of EN 1993-1-4 [9] for welded duplex and ferritic stainless steel I-section columns

Table 1: Material properties used to define the stress-strain response of duplex and ferritic stainless steel in this study

Stainless steel grade	$f_y$ (MPa)	$f_u$ (MPa)	$\epsilon_u$	$n$	$m$
Duplex	530	770	0.30	9.3	3.6
Ferritic	320	480	0.16	17.2	2.8

Table 2: Comparison of the ultimate strengths of duplex stainless steel I-section columns obtained in the experiments of [13, 15] and those determined through the finite element models of the specimens created in this study

Reference	Axis of buckling	Specimen ID	Cross-section	$L_{cr}$ (m)	$N_{ult,test}$ (kN)	$N_{ult,FE}$ (kN)	$\frac{N_{ult,test}}{N_{ult,FE}}$
Burgan et al. [15]	Major	C1	I160×160×6×8	1.93	1930	2167	0.89
		C2	I160×160×6×8	1.49	1490	1660	0.90
		C3	I160×160×6×8	0.99	990	1081	0.92
Yang et al. [13]	Major	I2205-2000	I150×150×6×10	2.38	1705	1768	0.96
		I2205-3000	I150×150×6×10	3.38	1366	1395	0.98
		I2205-3500	I150×150×6×10	3.88	1228	1236	0.99
		I2205-4000	I150×150×6×10	4.38	1065	1064	1.00
		I2205-4500	I110×150×6×10	4.88	619	546	1.13
	Minor	H2205-1500	I150×150×6×10	1.88	1470	1392	1.06
		H2205-2000	I150×150×6×10	2.38	1128	1098	1.03
		H2205-3000	I150×150×6×10	3.38	751	696	1.08
		H2205-3500	I150×150×6×10	3.88	677	578	1.17
		H2205-4000	I150×150×6×10	4.38	524	464	1.13
		H2205-4000-B	I150×120×6×10	4.38	321	252	1.27
		Average					
COV						0.11	

Table 3: Summary of parametric studies carried out in this paper

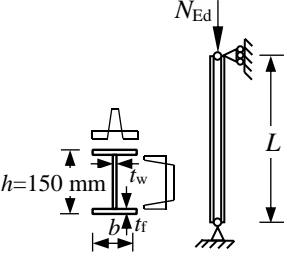
Loading condition	Cross-section aspect ratio $h/b$	Cross-section class	Axis of buckling	Stainless steel grade	$\bar{\lambda}$
	1.0	Class 1	Major Minor	Duplex Ferritic	0.1 to 2.5 with 10 different $L/h$ ratios
	1.5	Class 2			
	2.0	Class 3			
	3.0				

Table 4: Imperfection factor  $\alpha$  and threshold slenderness  $\bar{\lambda}_0$  values recommended by EN 1993-1-4 [9] for welded stainless steel I-section columns

Axis of buckling	$\alpha$	$\bar{\lambda}_0$
Major	0.49	0.20
Minor	0.76	0.20

Table 5: The values of the parameters  $\alpha$ ,  $\beta$ ,  $\lambda_0$ ,  $\lambda_1$  and  $E_0$  recommended by Australian & New Zealandian AS/NSZ 4673:2001 [11] for stainless steel columns

Coefficient	Duplex stainless steel (S31803)	Ferritic stainless steel (1.4003)
$\alpha$	1.16	0.94
$\beta$	0.13	0.15
$\lambda_0$	0.65	0.56
$\lambda_1$	0.42	0.27
$E_0$ (GPa)	200	195



Table 6: Accuracy of EN 1993-1-4 [9], AISC Design Guide 27 [12], ASCE/SEI-8 [10] and AS/NSZ 4673:2001 [11] for ultimate strength predictions of welded duplex and ferritic stainless steel I-section columns

Design method	Grade	Axis of buckling	N	$\epsilon_{av}$	$\epsilon_{COV}$	$\epsilon_{max}$	$\epsilon_{min}$
EN 1993-1-4 [9]	Duplex	Major	128	1.12	0.040	1.28	0.98
		Minor	126	1.16	0.044	1.47	1.04
	Ferritic	Major	120	1.11	0.051	1.26	1.00
		Minor	135	1.18	0.139	1.95	0.97
AISC Design Guide 27 [12]	Duplex	Major	128	1.39	0.176	1.81	0.99
		Minor	126	1.29	0.175	2.09	1.00
	Ferritic	Major	120	1.36	0.189	1.72	1.00
		Minor	135	1.33	0.242	2.62	0.95
ASCE/SEI-8 [10]	Duplex	Major	128	0.91	0.119	1.25	0.68
		Minor	126	0.83	0.147	1.21	0.66
	Ferritic	Major	120	0.90	0.124	1.26	0.72
		Minor	135	0.85	0.191	1.39	0.61
AS/NSZ 4673:2001 [11]	Duplex	Major	128	1.05	0.057	1.25	0.90
		Minor	126	0.96	0.077	1.22	0.68
	Ferritic	Major	120	1.05	0.059	1.26	0.92
		Minor	135	0.99	0.144	1.60	0.72

Table 7: Proposed imperfection factor  $\alpha$  and threshold slenderness  $\bar{\lambda}_0$  values for welded duplex and ferritic stainless steel I-section columns

Stainless steel grade	Axis of buckling	$\alpha$	$\bar{\lambda}_0$
Duplex	Major	0.49	0.30
	Minor	0.76	0.30
Ferritic	Major	0.42	0.20
	Minor	0.64	0.20

Table 8: Accuracy of the recalibrated column design method of EN 1993-1-4 [9] for welded duplex and ferritic stainless steel I-section columns

Design method	Grade	Axis of buckling	N	$\epsilon_{av}$	$\epsilon_{COV}$	$\epsilon_{max}$	$\epsilon_{min}$
Recalibrated EN 1993-1-4 [9]	Duplex	Major	128	1.09	0.050	1.26	0.93
		Minor	126	1.11	0.036	1.21	0.99
	Ferritic	Major	120	1.08	0.046	1.26	0.98
		Minor	135	1.13	0.137	1.85	0.97

Table 9: Reliability analysis of the recalibrated column design method of EN 1993-1-4 [9] for welded duplex and ferritic stainless steel I-section columns

Design method	Grade	Axis of buckling	Data	$N$	$b$	$k_{d,n}$	$V_\delta$	$\gamma_{M1}$
Recalibrated EN 1993-1-4 [9]	Duplex	Major	FE only	120	1.10	3.44	0.043	1.05
			Tests only	8	1.03	3.44	0.103	1.35
			Tests & FE	128	1.09	3.44	0.050	1.07
		Minor	FE only	120	1.11	3.44	0.036	1.03
			Tests only	6	1.29	3.44	0.088	1.05
			Tests & FE	126	1.12	3.44	0.053	1.05
	Ferritic	Major	FE only	120	1.08	3.44	0.049	1.03
			Tests only	—	—	—	—	—
			Tests & FE	—	—	—	—	—
		Minor	FE only	120	1.08	3.44	0.041	1.01
			Tests only	15	1.49	3.44	0.152	1.04
			Tests & FE	135	1.13	3.44	0.137	1.23

Table 10: Reliability analysis of the column design method of EN 1993-1-4 [9] for welded duplex and ferritic stainless steel I-section columns

Design method	Grade	Axis of buckling	Data	$N$	$b$	$k_{d,n}$	$V_\delta$	$\gamma_{M1}$
EN 1993-1-4 [9]	Duplex	Major	FE only	120	1.13	3.44	0.033	1.01
			Tests only	8	1.07	3.44	0.092	1.26
			Tests & FE	128	1.12	3.44	0.040	1.02
		Minor	FE only	120	1.15	3.44	0.026	0.97
			Tests only	6	1.33	3.44	0.072	0.97
			Tests & FE	126	1.16	3.44	0.044	1.00
	Ferritic	Major	FE only	120	1.11	3.44	0.051	1.00
			Tests only	—	—	—	—	—
			Tests & FE	—	—	—	—	—
		Minor	FE only	120	1.13	3.44	0.044	0.97
			Tests only	15	1.56	3.44	0.158	1.01
			Tests & FE	135	1.18	3.44	0.139	1.18